Chain Core Isomerism in dppm-Bridged Polymetallic Complexes. Synthesis, Reactivity, and Structure of Fe–Hg–Pt, Fe–Sn–Pt, and Fe–Pd–Sn Arrays (dppm = Ph₂PCH₂PPh₂)†

Pierre Braunstein,*,‡ Michael Knorr,‡ Martin Strampfer,‡
Antonio Tiripicchio,§ and Franco Ugozzoli§

Laboratoire de Chimie de Coordination, Associé au CNRS (URA 0416), Université Louis Pasteur, 4 rue Blaise Pascal, F-67070 Strasbourg Cédex, France, and Istituto di Chimica Generale ed Inorganica, Università di Parma, Centro di Studio per la Strutturistica Diffrattometrica del CNR, Viale delle Scienze, I-43100 Parma, Italy

The 14-electron fragment Pt(PPh₃)₂, delivered by [Pt(PPh₃)₂(C₂H₄)], selectively inserts into the Hg–C bond of the bimetallic complex [(OC)₃{(MeO)₃Si}Fe(μ-dppm)Hg(C₆Cl₅)] (2) (dppm = Ph₂PCH₂PPh₂) and quantitatively forms a 1:1 mixture of the isomeric complexes cis-[(OC)₃Fe{μ-Si(OMe)₂(OMe)}(μ-dppm)(μ-Hg)Pt(C₆Cl₅)(PPh₃)] (3) and trans-[(OC)₃Fe{μ-Si-(OMe)₂(OMe)}(μ-dppm)(μ-Hg)Pt(C₆Cl₅)(PPh₃)] (4) (in which the PPh₃ ligand is cis or trans relative to the Pt-bound phosphorus atom of the dppm ligand, respectively). Complex 3 was also obtained, selectively and in high yields, upon reaction of K[Fe{Si(OMe)₃}(CO)₃-(dppm-P)] with trans-[PtCl{Hg(C₆Cl₅)}(PPh₃)₂]. It readily isomerizes when heated in solution to quantitatively yield the thermodynamically more stable isomer 4. The geometry of 3 and 4 has been deduced from their reactivity and spectroscopic data. Reaction of [(OC)₃-{(MeO)₃Si}Fe(μ-dppm)PtH(PPh₃)] (5) with [Hg(C₆Cl₅)]PF₆ afforded the chloride-bridged cationic complex [(OC)₃Fe(μ-dppm)(μ-Cl)Pt(PPh₃)]PF₆ (6) and a small amount of 4. Two-electron donor ligands like isonitriles or CO displace the P(dppm)→Pt bond of 3, but not of 4, and selectively give chain complexes of the type [(OC)₃{(MeO)₃Si}Fe(μ-dppm)HgPt(C₆-Cl₅)(L)(PPh₃)] [L = (t-Bu)NC (7), (2,6-xylyl)NC (8), CO (9)]. Reaction of K[Fe{Si(OMe)₃}-(CO)₃(dppm-P)] with trans-[PtCl(SnCl₃)(PEt₃)₂] led to the stannylene-bridged complex [(OC)₃{(MeO)₃Si}Fe(μ-dppm)(μ-SnCl₂)PtCl(PEt₃)] (10) in high yields. Possible molecular rearrangements leading to the Fe–Sn–Pt sequence of 10 are discussed. Stirring a solution of [(OC)₃Fe{μ-Si(OMe)₂(OMe)}(μ-dppm)PdCl] with SnCl₂ yielded [(OC)₃Fe{μ-Si(OMe)₂(OMe)}-(μ-dppm)PdSnCl₃] (11) which contains a terminal SnCl₃ group, whereas the Pt analog could not be isolated. The solid state structures of 2, 7·CH₂Cl₂, and 10·CH₂Cl₂ have been determined by X-ray diffraction. 2 crystallizes in the monoclinic space group P2₁/a with Z = 4 in a unit cell of dimensions a = 20.943(8) Å, b = 16.612(7) Å, c = 11.837(5) Å, and β = 95.02(2)°. 7·CH₂Cl₂ crystallizes in the monoclinic space group P2₁/c with Z = 4 in a unit cell of dimensions a = 14.212(4) Å, b = 26.717(8) Å, c = 19.318(6) Å, and β = 117.58(2)°. 10·CH₂-Cl₂ crystallizes in the triclinic space group P1̄ with Z = 2 in a unit cell of dimensions a = 17.882(8) Å, b = 11.443(6) Å, c = 12.457(6) Å, α = 79.79(2), β = 88.18(2), and γ = 72.25(2)°. The structures have been solved from diffractometer data by Patterson and Fourier methods and refined by full-matrix least squares on the basis of 5363 (2), 2696 (7·CH₂Cl₂), and 10 339 (10·CH₂Cl₂) observed reflections to R and R' values of 0.0400 and 0.0464 (2), 0.0550 and 0.0357 (7·CH₂Cl₂), and 0.0494 and 0.0653 (10·CH₂Cl₂), respectively.

Introduction

Despite their relatively rare occurrence and sometimes difficult synthesis, the structural simplicity of metal–metal bonded, heterometallic chain complexes makes them good candidates for the study of the factors which govern their chemistry. Furthermore, the chemical diversity associated with heterometallic systems

(1) (a) Stone, F. G. A. *Angew. Chem., Int. Ed. Engl.* **1984**, *23*, 89. (b) Shriver, D. F.; Kaesz, H. D.; Adams, R. D. *The Chemistry of Metal Cluster Complexes*; VCH: Weinheim, 1990. (c) Vahrenkamp, H. *Adv. Organomet. Chem.* **1983**, *22*, 169. (d) Sappa, E.; Tiripicchio, A.; Braunstein, P. *Coord. Chem. Rev.* **1985**, *65*, 219. (e) Braunstein, P. In *Perspectives in Coordination Chemistry*; Williams, A. F., Floriani, C., Merbach, A. E., Eds.; Helvetica Chimica Acta Verlag and VCH Publishers: Basel and Weinheim, 1992; pp 67–107 (see also references cited therein).

constitutes a major characteristic which can be exploited to study the influence of a given metal on the structure and reactivity of the molecular ensemble.[1] Organometallic complexes with isomeric heterometallic cores should provide us with more comparable and detailed information about reactivity patterns and a better insight into the factors which govern their chemistry. Only few synthetic methods allow the selective access to m−Pt−m′ and m−m′−Pt arrangements (m, m′ = transition metal fragments), and virtually nothing is known about the possibility of interconverting positional isomers, whether by an intermolecular or intramolecular process. In previous investigations, three methods have been used to obtain complexes with m−Hg−Pt and m−Pt−Hg arrays. One method consists of the insertion reaction of the 14-electron, carbene-like Pt(PPh$_3$)$_2$ fragment into the Hg−carbon bond of bimetallic complexes of the type R−Hg−m (R = polyhaloaryl) (eq 1).[2a]

m = metal carbonyl fragment
R = polyhaloaryl group
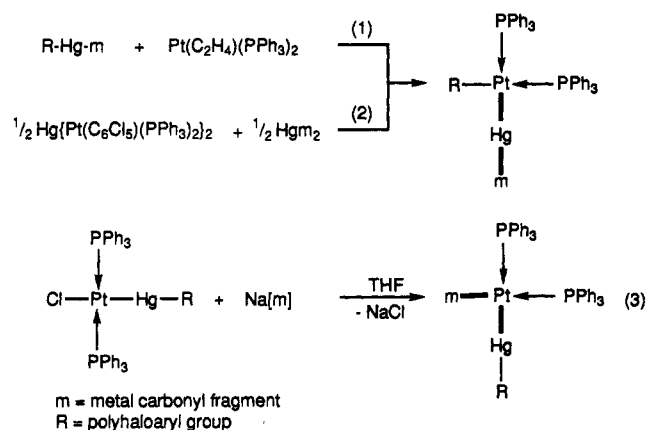
Another method consists of the double exchange (metathesis) reaction between complexes of the type m−Hg−m and R(PPh$_3$)$_2$Pt−Hg−Pt(PPh$_3$)$_2$R which yields the mixed-metal chains m−Hg−Pt (eq 2).[2c] Access to a positional isomer of the latter was recently found, whereby reaction of nucleophilic carbonyl metalates with *trans*-[PtCl(HgR)(PPh$_3$)$_2$] yielded m−Pt−Hg arrays (eq 3). With these new methods in hand, it has been possible to synthesize isomeric heterometallic chain complexes and relate their spectroscopic properties to the nucleophilicity of the metalates.[2d]

We described recently the use of the hydrido−silyl complexes [FeH{Si(OR)$_3$}(CO)$_3$(dppm-*P*)] and their derived metalates K[Fe{Si(OR)$_3$}(CO)$_3$(dppm-*P*)] (R = Me, Et; dppm = bis(diphenylphosphino)methane) for the rational synthesis of dppm-bridged, silicon-containing heterometallic arrays.[3a−m] The growing interest in complexes with transition metal-bound alkoxysilyl or siloxane ligands stems in part from their relevance as molecular models of silica surfaces.[4] The involvement of the silica surface in various catalytic processes using transition metals is far from being fully understood. Furthermore, there is a fundamental synthetic interest in metal-bound silyl groups. Such complexes may react by, e.g., insertion into the metal−silicon bond[5a] and silyl

transfer from a metal to a ligand[5b−l] or to another metal, as demonstrated recently.[3l,m] Silicon-containing heteropolymetallic systems have so far been only little studied, and we describe here the synthesis and unexpected properties of such complexes.

Experimental Section

All reactions were performed in Schlenk-tube flasks under purified nitrogen. Solvents were dried and distilled under nitrogen before use: tetrahydrofuran over sodium benzophenone−ketyl, toluene, benzene and hexane over sodium, dichloromethane from P$_2$O$_5$. Nitrogen (Air liquide, R-grade) was passed through BASF R3-11 catalyst and molecular sieve columns to remove residual oxygen or water. Elemental C, H, and N analyses were performed by the Service Central de Microanalyses du CNRS. Infrared spectra were recorded in the 4000−400-cm^{-1} region on Perkin-Elmer 398 and on Bruker IFS 66 spectometers. The FIR spectra were recorded on a Bruker IFS 113 optical device. The ^{1}H, ^{31}P{^{1}H}, and ^{199}Hg-{^{1}H} NMR spectra were recorded at 200.13, 81.02, and 35.8 MHz, respectively, on a Bruker SY200 instrument. Phosphorus chemical shifts were externally referenced to 85% H$_3$PO$_4$ in H$_2$O with downfield chemical shifts reported as positive. Mercury chemical shifts were externally referenced to HgMe$_2$ in benzene with downfield chemical shifts reported as positive. Mass spectra were measured on a Fisons ZAB-HF spectrometer (Université Louis Pasteur, R. Hueber). The reactions were generally monitored by IR in the ν(CO) region. K[Fe-(CO)$_3${Si(OMe)$_3$}(dppm-*P*)],[3e] *trans*-[PtCl{Hg(C$_6$Cl$_5$)}(PPh$_3$)$_2$],[6]

mer-[(OC)$_3${(MeO)$_3$Si}Fe(μ-dppm)Hg(C$_6$Cl$_5$)],[3f]   *mer*-[(OC)$_3$-{(MeO)$_3$Si}Fe(μ-dppm)PtH(PPh$_3$)},[3a] *mer*-[(OC)$_3$Fe{μ-Si(OMe)$_2$-

(3) (a) Braunstein, P.; Knorr, M.; Tiripicchio, A.; Tiripicchio-Camellini, M. *Angew. Chem., Int. Ed. Engl.* **1989**, *28*, 1361. (b) Braunstein, P.; Knorr, M.; Villarroya, E.; Fischer, J. *New J. Chem* **1990**, *14*, 583. (c) Braunstein, P.; Knorr, M.; Piana, H.; Schubert, U. *Organometallics* **1991**, *10*, 828. (d) Braunstein, P.; Knorr, M.; Villarroya, E.; DeCian, A.; Fischer, J. *Ibid.* **1991**, *10*, 3714. (e) Braunstein, P.; Knorr, M.; Schubert, U.; Lanfranchi, M.; Tiripicchio, A. *J. Chem. Soc., Dalton Trans.* **1991**, 1507. (f) Braunstein, P.; Douce, L.; Knorr, M.; Strampfer, M.; Lanfranchi, M.; Tiripicchio, A. *Ibid.* **1992**, 331. (g) Braunstein, P.; Colomer, E.; Knorr, M. Tiripicchio, A.; Tiripicchio-Camellini, M. *Ibid.* **1992**, 903. (h) Reinhard, G.; Hirle, B.; Schubert, U.; Knorr, M.; Braunstein, P.; DeCian, A.; Fischer, J. *Inorg. Chem.* **1993**, *32*, 1656. (i) Balegroune, F.; Braunstein, P.; Douce, L.; Dusausoy, Y.; Grandjean, D.; Knorr, M.; Strampfer, M. *J. Cluster Sci.* **1992**, *3*, 275. (j) Knorr, M.; Braunstein, P. *Bull. Soc. Chim. Fr.* **1992**, *129*, 663. (k) Braunstein, P.; Knorr, M.; Tiripicchio, A.; Tiripicchio-Camellini, M. *Inorg. Chem.* **1992**, *31*, 3685. (l) Braunstein, P.; Knorr, M.; Hirle, B.; Reinhard, G.; Schubert, U. *Angew. Chem., Int. Ed. Engl.* **1992**, *31*, 1583. (m) Reinhard, G.; Knorr M.; Braunstein, P.; Schubert, U.; Khan, S.; Strouse, C. E.; Kaesz, H. D.; Zinn, A. *Chem. Ber.* **1993**, *126*, 17. (n) Braunstein, P.; Richert, J.-L.; Dusausoy, Y. *J. Chem. Soc., Dalton Trans.* **1990**, 3801. (o) Knorr, M.; Faure, T.; Braunstein, P. *J. Organomet. Chem.* **1993**, *447*, C4. (p) Schubert, U.; Gilbert, S.; Knorr, M. *Ibid.* **1993**, *454*, 79.

(4) (a) Winkhofer, N.; Roesky, H. W.; Noltemeyer, M.; Robinson, W. T.; *Angew. Chem., Int. Ed. Engl.* **1992**, *31*, 599. (b) Feher, F. J. *J. Am. Chem. Soc.* **1986**, *108*, 3850 and references cited therein.

(5) (a) Tilley, T. D. In *The Chemistry of Organic Silicon Compounds*; Patai, S., Rappoport, Z., Eds.; John Wiley & Sons: New York, 1988; Chapter 26. (b) Harris, P. J.; Howard, J. A. K.; Knox, S. A. R.; McKinney, R. J.; Phillips, R. P.; Stone, F. G. A.; Woodward, P. *J. Chem. Soc., Dalton Trans.* **1978**, 403. (c) Thum, G.; Ries, W.; Greissinger, D.; Malisch, W. *J. Organomet. Chem.* **1983**, *252*, C67. (d) Brinkman, K. C.; Blakeney, A. J.; Krone-Schmidt, W.; Gladysz, J. A. *Organometallics* **1984**, *3*, 1325. (e) Schubert, U.; Schenkel, A.; Müller, J. *J. Organomet. Chem.* **1985**, *292*, C11. (f) Pasman, P.; Snel, J. J. M. *Ibid.* **1986**, *301* 329. (g) Schubert, U.; Schenkel, A. *Chem. Ber.* **1988**, *121*, 939. (h) Crocco, G. L.; Young, C. S.; Lee, K. E.; Gladysz, J. A. *Organometallics* **1988**, *7*, 2158. (i) Ojima, I.; Clos, N. Donovan R. J. Ingallina, P. *Organometallics* **1990**, *9*, 3127. (j) Ojima, I.; Ingallina, P.; Donovan, R. J.; Clos, N. *Ibid.* **1991**, *10*, 38. (k) Ojima, I.; Donovan, R. J.; Clos, N. *Ibid.* **1991**, *10*, 2606. (l) Adams, R. D.; Cortopassi, J. E.; Pompeo, M. P. *Ibid.* **1992**, *11*, 1. (m) For a −SiMe$_3$ migration from Si to Pt, see: Chang, L. S.; Johnson, M. P.; Fink, M. J. *Ibid.* **1989**, *8*, 1369.

(6) Calvet, J.; Rossell, O.; Seco, M. *Transition Met. Chem.* **1984**, *9*, 208.

(2) (a) Braunstein, P.; Rossell, O.; Seco, M.; Torra, I.; Solans, X.; Miravitlles, C. *Organometallics* **1986**, *5*, 1113. (b) Rossell, O.; Seco, M.; Braunstein, P. *J. Organomet. Chem.* **1984**, *273*, 233. (c) Rossell, O.; Seco, M.; Torra, I. *J. Chem. Soc., Dalton Trans.* **1986**, 1011. (d) Calvet, J.; Rossell, O.; Seco, M.; Braunstein, P. *J. Chem. Soc., Dalton Trans.* **1987**, *119*.

(OMe)}(μ-dppm)PdCl],[3a] and *trans*-[PtCl(SnCl₃)(PEt₃)₂][7] were prepared according to the literature.

mer-[(OC)₃{(MeO)₃Si}Fe(μ-dppm)Hg(C₆Cl₅)] (2). Synthesis and data were as described previously.[3f] Crystals suitable for X-ray analysis were obtained by slow diffusion of hexane into a chlorobenzene solution of **2**. NMR: ¹⁹⁹Hg{¹H} (35.8 MHz, CH₂Cl₂/C₆D₆) δ −584 (dd, ¹J(Hg−P) = 558, ²J(Hg−P) = 242 Hz).

cis-[(OC)₃Fe{μ-Si(OMe)₂(OMe)}(μ-dppm)(μ-Hg)Pt(C₆-Cl₅)(PPh₃)] (3). A solution of K[Fe(CO)₃{Si(OMe)₃}(dppm-P)] (0.343 g, 0.50 mmol) in THF (20 mL) was slowly added at −30 °C to a solution of *trans*-[PtCl{Hg(C₆Cl₅)}(PPh₃)₂] (0.663 g, 0.55 mmol) in THF (10 mL). After warming to room temperature, the reaction mixture was stirred for 30 min; then the orange solution was filtered through Celite and the volume of solvent was reduced to 5 mL. Addition of hexane led to the precipitation of air-stable, bright yellow, and microcrystalline **3**. The filtrate was left standing for 12 h at −30 °C and yielded a second crop of the product (total yield: 0.660 g, 85%). (Anal. Calc for C₅₅H₄₆Cl₅HgFeO₆P₃PtSi (M = 1552.76): C, 42.54; H, 2.99. Found: C, 42.69; H, 3.12.) IR, ν(CO): (THF) 1991 (s), 1936 (s), 1918 (vs) cm⁻¹; (CH₂Cl₂) 1990 (s), 1930 (sh), 1915 (vs) cm⁻¹. NMR: ¹H (200 MHz, CD₂Cl₂) δ 3.02 (t, 2H, CH₂, ²J(P−H) = 10, ³J(H−¹⁹⁵Pt) = 40), 3.42 (s, 9H, OCH₃), 6.75−7.45 (m, 35H, C₆H₅); ³¹P{¹H} (81.02 MHz, THF/C₆D₆) δ 52.9 (d, P¹(Fe), ²⁺⁴J(P¹−P²) = 8, ²J(P¹−¹⁹⁹Hg) = 317, ³J(P¹−¹⁹⁵Pt) = 20), 38.2 (d, P³(Pt), ²J(P²−P³) = 11, ¹J(P³−¹⁹⁵Pt) = 2818, ²J(P³−¹⁹⁹Hg) not detected (masked)), 9.9 (dd, P²(Pt), ¹J(P²−¹⁹⁵Pt) = 2532, ²J(P²−¹⁹⁹Hg) = 551); ¹⁹⁹Hg{¹H} (35.8 MHz, toluene/C₆D₆, 273 K) δ −308 (ddd, ²J(Hg−P³) = 2867, ²J(Hg−P²) = 547, ²J(Hg−P¹) = 308, ¹J(Hg−¹⁹⁵Pt) = ca. 11 000 Hz).

trans-[(OC)₃Fe{μ-Si(OMe)₂(OMe)}(μ-dppm)(μ-Hg)Pt-(C₆Cl₅)(PPh₃)] (4). A THF or toluene solution (10 mL) of **3** (0.776 g, 0.50 mmol) was stirred at 70 °C for 3 h. The resulting orange solution was cooled to room temperature and was filtered to remove traces of elemental mercury. The solvent was evaporated under vacuum, and the residue consisting of pure **4** was washed with hexane. **4** is soluble in ether and other organic solvents and slightly soluble in hexane (0.70 g, 90%). (Anal. Calc. for C₅₅H₄₆Cl₅HgFeO₆P₃PtSi·2C₆H₅Cl (M = 1552.76 + 225.12): C, 45.26; H, 3.175. Found: C, 45.03; H, 3.04.) IR (THF), ν(CO): 1985 (s), 1926 (s), 1906 (vs) cm⁻¹. NMR: ¹H (200 MHz, C₆D₆) δ 3.17 (dt, 2H, CH₂, ²J(P−H) = 10, ⁴J(P−H) = 2, ³J(H−¹⁹⁵Pt) = 45), 3.49 (s, 9H, OCH₃), 6.73−7.87 (m, 35H, C₆H₅); ³¹P{¹H} (81.02 MHz, THF/C₆D₆) (ABX spin system) (J(P−P) and J(P−¹⁹⁵Pt) coupling constants determined by spectral simulation) δ 57.2 (P¹(Fe), ⁴J(P¹−P³) = −0.8, ²⁺⁴J(P¹−P²) = 10.6, ²J(P¹−¹⁹⁹Hg) = 200, ³J(P¹−¹⁹⁵Pt) = 9), 26.9 (P³(Pt), PPh₃, ²J(P³−P²) = 391.0, ¹J(P³−¹⁹⁵Pt) = 3200, ²J(P³−¹⁹⁹Hg) = 220), 18.6 (P²(Pt), dppm, ¹J(P²−¹⁹⁵Pt) = 2907, ²J(P²−¹⁹⁹Hg) = 540); ¹⁹⁹Hg{¹H} (35.8 MHz, toluene/C₆D₆, 312 K) δ −83 (dt, ²J(Hg−P¹) = ²J(Hg−P³) = 215, ²J(Hg−P²) = 547, ¹J(Hg−¹⁹⁵Pt) = 6320 Hz).

[(OC)₃Fe(μ-dppm)(μ-Cl)Pt(PPh₃)]PF₆ (6). A suspension of [HgCl(C₆Cl₅)] (0.088 g, 0.18 mmol) and TlPF₆ (0.064 g, 0.18 mmol) in CH₂Cl₂ (5 mL) was stirred for 24 h at room temperature and filtered (solution A). A cold solution (B) of [(OC)₃{(MeO)₃Si}Fe(μ-dppm)Pt(H)(PPh₃)] (5) (0.200 g, 0.18 mmol) in CH₂Cl₂ (10 mL) was added to solution A at −30 °C. The mixture turned yellow, and upon warming to room temperature, the color changed to deep red. After filtration the solvent was evaporated to 2 mL. Slow diffusion of hexane (10 mL) into the solution at 10 °C yielded dark red crystals of **6** (0.145 g, 70%). When the order of addition of the reagents was reversed, i.e. a cold solution A was added to solution B at −30 °C, less **6** was formed; instead the reaction mixture contained 25% of **4**. (Anal. Calc for C₄₆H₃₇ClF₆FeO₃P₄Pt (M

(7) Pregosin, P. S.; Sze, S. N. *Helv. Chim. Acta* **1978**, *61*, 1848.

= 1162.07): C, 47.55; H, 3.21. Found: C, 47.47; H, 3.15.) MS FAB⁺ (*m*-O₂N−C₆H₄−CH₂OH (NBA), THF) (M(monoisotopic) = 1016.06): *m/e* 1016.6 (M⁺), 932.6 (M⁺ − 3CO), 1088.6 (M⁺ + THF), 1003.6 (M⁺ + THF − 3CO). IR, ν(CO): (CH₂Cl₂) 2055 (s), 2007 (s), 1986 (vs) cm⁻¹; (KBr): 2043 (s), 1999 (vs), 1978 (vs) cm⁻¹. IR, ν(PF₆): (KBr) 841 (vs) cm⁻¹. FIR (polyethylene): 354 (s) cm⁻¹. NMR: ¹H (200 MHz, CD₂Cl₂) δ 4.47 (t, 2H, CH₂, ²J(H−P) = 11.4, ³J(H−¹⁹⁵Pt) = 61), 7.10−7.70 (m, 35H, C₆H₅); ³¹P{¹H} (81.02 MHz, CH₂Cl₂/C₆D₆) δ 64.6 (dd, P¹-(Fe), J(P¹−P³) = 37, J(P¹−P²) = 20, ²J(P−¹⁹⁵Pt) not resolved), 30.6 (dd, PPh₃, ²J(P−P) = 18, ¹J(P−¹⁹⁵Pt) = 2970), 2.2 (t, P² (Pt), ¹J(P²−¹⁹⁵Pt) = 4717), −152.4 (sept, PF₆, ¹J(P−F) = 711 Hz).

mer-[(OC)₃{(MeO)₃Si}Fe(μ-dppm)HgPt(C₆Cl₅)(t-BuNC)-(PPh₃)] (7). Pure *t*-BuNC (0.042 g, 0.50 mmol) was added via microsyringe to a toluene solution (10 mL) of **3** (0.776 g, 0.50 mmol) at −30 °C. The resulting solution was warmed to room temperature and stirred for 1 h. The yellowish solution was filtered to remove traces of elemental mercury. The solvent was evaporated to 2 mL, and hexane was layered over the solution. Crystallization at 5 °C yielded bright yellow crystals. Suitable crystals for X-ray analysis were obtained by slow diffusion of hexane into a chlorobenzene solution of **7** (0.532 g, 65%). (Anal. Calc for C₆₀H₅₅Cl₅FeHgNO₆P₃PtSi (M = 1635.895): C, 44.05; H, 3.39; N, 0.86. Found: C, 43.80; H, 3.44; N, 0.72.) IR (CH₂Cl₂): ν(CN) 2170 (m) cm⁻¹, ν(CO) 1983 (m), 1928 (vs), 1908 (sh) cm⁻¹. NMR: ¹H (200 MHz, C₆D₆) δ 0.87 (s, 9H, CCH₃), 3.37 (dd, 2H, CH₂, ²J(H−P) = 9.1 and 2.7), 4.03 (s, 9H, OCH₃) 6.95−7.64 (m, 35H, C₆H₅); ³¹P{¹H} (81.02 MHz, CH₂Cl₂/C₆D₆), δ 54.5 (dd, P¹(Fe), ²⁺³J(P¹−P²) = 96, ⁴⁺⁵J(P¹−P³) = 5.7, ²⁺³J(P²−¹⁹⁹Hg) = 100, ³⁺⁴J(P¹−¹⁹⁵Pt) = 35), 28.7 (dd, P³(Pt), ¹J(P³−¹⁹⁵Pt) = 2350, ²J(P³−¹⁹⁹Hg) = 2970), −25.4 (dd, P², ³J(P²−P³) = 7.2, ¹J(P²−¹⁹⁹Hg) = 210, ²J(P²−¹⁹⁵Pt) = 35); ¹⁹⁹Hg{¹H} (35.8 MHz, THF/toluene-d₈) δ −753 (ddd, ²J(Hg−P¹) = 100, ¹J(Hg−P²) = 215, ²J(Hg−P³) = ca. 3000 Hz).

mer-[(OC)₃{(MeO)₃Si}Fe(μ-dppm)HgPt(C₆Cl₅){(2,6-xylyl)NC}(PPh₃)] (8) was synthesized similarly to **7** by using **3** (0.776 g, 0.50 mmol) and (2,6-xylyl)NC (0.066 g, 0.50 mmol) (yield 0.51 g, 60%). (Anal. Calc for C₆₄H₅₅Cl₅FeHgNO₆P₃PtSi (M = 1683.94): C, 45.65; H, 3.29. Found: C, 45.72, H, 3.42.) IR (CH₂Cl₂): ν(CN) 2137 (s) cm⁻¹; ν(CO) 1987 (s), 1926 (sh), 1913 (vs) cm⁻¹. NMR: ¹H (200 MHz, C₆D₆) δ 1.97 (s, 6H, PhCH₃), 3.36 (dd, 2H, CH₂, ²J(H−P) = 9.5 and ca. 2), 3.92 (s, 9H, OCH₃), 6.47−7.86 (m, 38H, C₆H₅); ³¹P{¹H} (81.02 MHz, CH₂Cl₂/C₆D₆) δ 54.7 (dd, P¹(Fe), ²⁺³J(P¹−P²) = 93, ⁴⁺⁵J(P¹−P³) = 6, ²⁺³J(P²−¹⁹⁹Hg) = ca. 100, ³⁺⁴J(P¹−¹⁹⁵Pt) = ca. 35), 30.5 (dd, P³(Pt), ¹J(P³−¹⁹⁵Pt) = 2370, ²J(P³−¹⁹⁹Hg) = 2830), −27.5 (dd, P², ³J(P³−P²) = 6, ²J(P²−¹⁹⁵Pt) ca. 35, ¹J(P²−¹⁹⁹Hg) = ca. 170 Hz).

mer-[(OC)₃{(MeO)₃Si}Fe(μ-dppm)HgPt(C₆-Cl₅)(CO)(PPh₃)] (9). CO was bubbled for 1 min through a CH₂Cl₂ solution (10 mL) of **3** (0.776 g, 0.50 mmol). The solution was stirred under a CO atmosphere for 30 min. The resulting yellowish solution was filtered to remove some elemental Hg and evaporated under reduced pressure to 2 mL. Addition of hexane (10 mL) and standing at −30 °C yielded **9** as a yellow powder (0.51 g, 65%). No satisfactory microanalysis could be obtained. IR, ν(CO): (CH₂Cl₂) 2042 (ms), 1993 (s), 1932 (sh), 1923 (vs) cm⁻¹; (KBr) 2045 (m), 1990 (s), 1925 (vs br) cm⁻¹. NMR: ¹H (200 MHz, CDCl₃) δ 2.98 (t, 2H, CH₂, ²J(H−P) = 9.7, ⁴J(H−¹⁹⁵Pt) = 32), 3.49 (s, 9H, OCH₃), 6.74−7.45 (m, 35H, C₆H₅); ³¹P{¹H} (81.02 MHz, CH₂Cl₂/C₆D₆) δ 53.3 (dd, P¹(Fe), ²⁺³J(P¹−P²) = 101, ⁴⁺⁵J(P¹−P³) = 5, ²⁺³J(P¹−¹⁹⁹Hg) = ca. 80, ³⁺⁴J(P¹−¹⁹⁵Pt) = 33), 36.5 (dd, P³(Pt), ³J(P³−P²) = 6, ¹J(P³−¹⁹⁵Pt) = 2213, ²J(P³−¹⁹⁹Hg) not determined), −25.3 (dd, P², ²J(P²−¹⁹⁵Pt) = 43, ¹J(P²−¹⁹⁹Hg) = ca. 270 Hz).

mer-[(OC)₃{(MeO)₃Si}Fe(μ-dppm)(μ-SnCl₂)PtCl-(PEt₃)] (10). A solution of K[Fe(CO)₃{Si(OMe)₃}(dppm-P)] (0.343 g, 0.50 mmol) in THF (20 mL) was slowly added at −30 °C to a solution of *trans*-[PtCl(SnCl₃)(PEt₃)₂] (0.333 g, 0.55

Table 1. Crystal Data and Data Collection Parameters^a for the Complexes 2, 7·CH$_2$Cl$_2$, and 10·CH$_2$Cl$_2$

	2	7·CH$_2$Cl$_2$	10·CH$_2$Cl$_2$
formula	C$_{37}$H$_{31}$Cl$_5$FeHgO$_6$P$_2$Si	C$_{60}$H$_{55}$Cl$_5$FeHgNO$_6$P$_3$PtSi·CH$_2$Cl$_2$	C$_{37}$H$_{46}$Cl$_3$FeO$_6$P$_3$PtSiSn·CH$_2$Cl$_2$
M	1095.38	1720.83	1268.69
cryst syst	monoclinic	monoclinic	triclinic
space group	P2$_1$/a	P2$_1$/c	P$\bar{1}$
a, Å	20.943(8)	14.212(4)	17.882(8)
b, Å	16.612(7)	26.717(8)	11.443(6)
c, Å	11.837(5)	19.318(6)	12.457(6)
α, deg	90	90	79.79(2)
β, deg	95.02(2)	117.58(2)	88.18(2)
γ, deg	90	90	72.25(2)
V, Å^3	4102(3)	6502(4)	2389(2)
Z	4	4	2
D$_c$, g cm^{-3}	1.773	1.758	1.764
F(000)	2144	3360	1244
cryst dimens, mm	0.18 × 0.24 × 0.28	0.10 × 0.16 × 0.24	0.25 × 0.28 × 0.35
μ(Mo Kα), cm^{-1}	45.68	51.74	42.19
diffractometer	Philips PW 1100	Siemens AED	Siemens AED
2θ range, deg	6–54	6–48	6–62
reflns measd	±h,k,l	±h,k,l	±h,±k,l
max, min transm factors	1.294–0.739	1.421–0.838	1.554–0.696
unique reflns	9002	7603	15 222
obsd reflns [I > 2σ(I)]	5363	2696	10 339
R	0.0400	0.0550	0.0494
R′	0.0464	0.0357	0.0653

^{a} Details in common: T = 295 K; Mo Kα radiation (λ = 0.710 73 Å); $\theta/2\theta$ scan mode; $(\theta - 0.6) - (\theta + 0.6 + 0.346 \tan \theta)°$ scan width; 2.5–12°·min^{-1} scan speed; one standard reflection measured after 50 reflections.

mmol) in THF (10 mL). After stirring at 0 °C for 0.5 h, the resulting mixture was filtered over Celite. The solvent was evaporated to dryness, and the yellow residue was dissolved in 3 mL of cold CH$_2$Cl$_2$. The solution was filtered again and two equivalent volumes of hexane were added. After standing at −30 °C the solution yielded bright yellow, crystalline 10. Crystals suitable for X-ray analysis were obtained by slow diffusion of hexane into a CH$_2$Cl$_2$ solution of 10 at −30 °C (0.414 g, 70%). (Anal. Calc for C$_{37}$H$_{46}$Cl$_3$FeO$_6$P$_3$PtSiSn·CH$_2$-Cl$_2$ (M = 1183.775 + 84.93): C, 35.98; H, 3.81. Found: C, 35.71; H, 3.87.) MS FAB$^+$ (NBA, THF) (M(monoisotopic) = 1182.936): m/e 1148.7 (M$^+$ − Cl), 958 (M$^+$ − Cl − SnCl$_2$), 944.7 (M$^+$ − Sn − Cl − 3CO), 909.9 (944.7 − Cl), 873.9 (958 − 3CO), 850.9 (944.7 − Si(OMe)$_3$ + CO + H), 818 (850.9 − Cl), 789 (909.9 − Si(OMe)$_3$), 754 (789 − Cl). IR, ν(CO): (THF) 2037 (m), 1985 (s), 1967 (vs) cm^{-1}; (KBr) 2036 (s), 1989 (s), 1966 (vs) cm^{-1}. FIR (polyethylene): 350 (s), 311 (s), 281 (vs br), 225 (s) cm^{-1}. NMR: ^{1}H (200 MHz, CDCl$_3$) δ 1.18 (m, 9H, CH$_3$), 2.32 (m, 6H, PCH$_2$), 3.62 (br, 2H, PCH$_2$P), 3.70 (s, 9H, OCH$_3$), 7.26–7.62 (m, 20H, C$_6$H$_5$); ^{31}P{^{1}H} (81.02 MHz, CH$_2$Cl$_2$/C$_6$D$_6$, 263 K) (ABX spin system) (P–P coupling constants determined by spectral simulation) δ 37.0 (P(Fe), ^{2+4}J(P^1–P^2) = 27.4, ^4J(P^1–P^3) = 0.4 ^3J(P^1–^{195}Pt) = ca. 10, ^2J(P^1–^{117,119}Sn) = 200), 15.2 (P^3(Pt), ^2J(P^3–P^2) = 366.8, ^1J(P^3–^{195}Pt) = 2640, ^2J(P^3–^{117,119}Sn) = 130), 11.0 (P^2(Pt), ^2J(P^2–^{195}Pt) = 2316, ^2J(P^2–^{117,119}Sn) = 205 Hz).

mer-[(OC)$_3$Fe{μ-Si(OMe)$_2$(OMe)}(μ-dppm)PdSnCl$_3$] (11). Solid SnCl$_2$ (0.095 g, 0.50 mmol) was added to a dark red CH$_2$-Cl$_2$ solution (10 mL) of [(OC)$_3$Fe{μ-Si(OMe)$_2$(OMe)}(μ-dppm)-PdCl] (0.394 g, 0.50 mmol), and the mixture was stirred for 24 h. The solution turned darker with time. It was filtered, and the same volume of hexane was added to yield a dark oily residue which was eliminated. The solution was concentrated to 10 mL and was left standing at 30 °C overnight, and red crystals were formed (0.290 g, 60%). (Anal. Calc for C$_{31}$H$_{31}$-Cl$_3$FeO$_6$P$_2$PdSiSn (M = 976.96): C, 38.11; H, 3.20. Found: C, 39.83; H, 3.13.) IR (CH$_2$Cl$_2$), ν(CO): 1994 (m), 1938 (s), 1926 (s) cm^{-1}. FIR (polyethylene): 383 (w), 351 (w), 321 (vs), 308 (s), 304 (s), 269 (m), 225 (w), 202 (w) cm^{-1}. NMR: ^{1}H (200 MHz, CD$_2$Cl$_2$, 298 K) δ 3.81 (s, 9H, OCH$_3$), 4.07 (dd, 2H, PCH$_2$P, ^2J(P–H) = 11.5 and 10.2), 7.32–7.75 (m, 20H, C$_6$H$_5$); ^{1}H (200 MHz, CDCl$_2$ 193 K) δ 3.61, 3.65, 3.69 (s, 9H, OMe);

^{31}P{^{1}H} (81.02 MHz, CH$_2$Cl$_2$/C$_6$D$_6$) δ 43.8 (d, P(Fe), ^{2+3}J(P–P) = 52 Hz), 30.6 (d, P(Pd)).

X-ray Crystal Structure Determinations. The crystal data and data collection parameters for *mer*-[(OC)$_3${(MeO)$_3$Si}-Fe(μ-dppm)Hg(C$_6$Cl$_5$)] (2), *mer*-[(OC)$_3${(MeO)$_3$Si}Fe(μ-dppm)-HgPt(C$_6$Cl$_5$)(t-BuNC)(PPh$_3$)]·CH$_2$Cl$_2$ (7·CH$_2$Cl$_2$), and *mer*-[(OC)$_3${(MeO)$_3$Si}Fe(μ-dppm)(μ-SnCl$_2$)PtCl(PEt$_3$)]·CH$_2$Cl$_2$ (10·CH$_2$Cl$_2$) are summarized in Table 1. An empirical correction for absorption was applied.[8a,b] Only the observed reflections were used in the structure solution and refinement.

The structures were solved by Patterson and Fourier methods. From the ΔF maps of 7 and 10 the presence of a dichloromethane molecule of solvation was revealed (with a chlorine atom disordered in two positions in 10). The refinements were carried out by full-matrix least squares first with isotropic and then with anisotropic thermal parameters in the last cycles for all the non-hydrogen atoms (2), for all the non-hydrogen atoms except the carbon atoms (7), and for all the non-hydrogen atoms except the atoms of the solvent (10). All hydrogen atoms (except those of the solvent molecule in 10) were placed at their geometrically calculated positions and refined "riding" on the corresponding carbon atoms. In the final cycles of refinement a weighting scheme, $w = [\sigma^2(F_o) + gF_o^2]^{-1}$ was used; at convergence the g values were 0.0012 (2), 0 (7·CH$_2$Cl$_2$), and 0.0024 (10·CH$_2$Cl$_2$), respectively. The atomic scattering factors, corrected for the real and imaginary parts of anomalous dispersion, were taken from ref 8c.

All calculations were carried out on the GOULD POWER-NODE 6040 of the "Centro di Studio per la Strutturistica Diffrattometrica" del CNR, Parma, using the SHELX-76 and SHELXS-86 systems of crystallographic computer programs.[9] The final atomic coordinates for the non-hydrogen atoms are given in Tables 2 (2), 3 (7·CH$_2$Cl$_2$), and 4 (10·CH$_2$Cl$_2$).

(8) (a) Walker, N.; Stuart, D. *Acta Crystallogr., Sect. A* **1983**, *39*, 158. (b) Ugozzoli, F. *Comput. Chem.* **1987**, *11*, 109. (c) *International Tables for X-Ray Crystallography*; Kynoch Press: Birmingham, England, 1974; Vol. IV.

(9) (a) Sheldrick, G. M. SHELX-76 Program for crystal structure determination. University of Cambridge, England, 1976. (b) Sheldrick, G. M. SHELXS-86 Program for the solution of crystal structures. University of Göttingen, 1986.

Table 2. Fractional Atomic Coordinates ($\times 10^4$) and Equivalent Isotropic Thermal Parameters ($\text{Å}^2 \times 10^4$) with Esd's in Parentheses for the Non-Hydrogen Atoms of [(MeO)$_3$Si)(OC)$_3$Fe(μ-dppm)Hg(C$_6$Cl$_5$)] (2)

|	x/a	y/b	z/c	$U_{eq}{}^a$		x/a	y/b	z/c	$U_{eq}{}^a$
Hg	2913(1)	374(1)	4445(1)	432(1)	C(12)	4214(3)	1249(5)	4502(6)	471(26)
Fe	1763(1)	−38(1)	4612(1)	408(3)	C(13)	3255(3)	1063(4)	1368(6)	450(24)
Cl(1)	3814(1)	−890(1)	3200(2)	734(9)	C(14)	3768(4)	1573(5)	1718(7)	547(28)
Cl(2)	5227(1)	−659(2)	2683(2)	985(11)	C(15)	4364(4)	1490(6)	1306(8)	658(34)
Cl(3)	5958(1)	893(2)	3485(2)	1100(13)	C(16)	4463(4)	881(6)	549(8)	764(39)
Cl(4)	5257(1)	2232(2)	4728(3)	1063(12)	C(17)	3978(5)	376(6)	200(8)	766(39)
Cl(5)	3813(1)	2012(1)	5129(2)	764(9)	C(18)	3381(4)	463(5)	613(7)	629(31)
Si	1995(1)	−11(2)	6557(2)	560(8)	C(19)	2030(3)	1836(4)	1075(7)	465(26)
P(1)	2520(1)	1188(1)	2063(2)	475(7)	C(20)	2017(4)	1809(5)	−94(7)	651(34)
P(2)	1525(1)	−67(1)	2716(2)	391(6)	C(21)	1669(4)	2332(6)	−767(8)	738(38)
O(1)	1643(3)	1703(4)	4847(6)	822(27)	C(22)	1294(5)	2879(6)	−133(9)	819(42)
O(2)	2400(3)	−1612(4)	4672(7)	954(32)	C(23)	1271(5)	2916(5)	846(10)	883(45)
O(3)	525(3)	−659(4)	5126(5)	712(23)	C(24)	1652(4)	2399(5)	1541(8)	713(36)
O(4)	2724(3)	205(5)	6985(7)	1101(37)	C(25)	844(3)	534(4)	2114(6)	409(24)
O(5)	1856(4)	−896(4)	7107(5)	1000(32)	C(26)	708(4)	570(5)	944(6)	554(29)
O(6)	1607(3)	640(4)	7257(5)	416(24)	C(27)	188(4)	1003(5)	499(7)	648(33)
C(1)	1699(4)	1028(5)	4756(7)	544(30)	C(28)	−200(4)	1381(5)	1165(8)	663(33)
C(2)	2150(4)	−985(5)	4646(7)	635(33)	C(29)	−78(4)	1350(5)	2316(8)	709(35)
C(3)	1003(3)	−404(4)	4916(6)	482(25)	C(30)	449(4)	932(4)	2804(7)	533(28)
C(4)	2977(5)	900(8)	7461(10)	1299(62)	C(31)	1280(3)	−1058(4)	2203(6)	435(24)
C(5)	1979(8)	−1098(11)	8263(12)	1722(87)	C(32)	699(4)	−1356(4)	2463(6)	551(29)
C(6)	977(5)	742(8)	7243(11)	1183(60)	C(33)	483(4)	−2114(5)	2110(7)	654(33)
C(7)	3891(3)	561(4)	4200(6)	405(23)	C(34)	847(5)	−2581(5)	1499(7)	740(39)
C(8)	4220(3)	−21(5)	3642(6)	462(25)	C(35)	1418(6)	−2303(5)	1218(8)	840(43)
C(9)	4846(4)	76(5)	3411(7)	563(29)	C(36)	1653(4)	−1544(5)	1576(7)	680(35)
C(10)	5172(4)	759(6)	3770(7)	635(32)	C(37)	2157(4)	173(4)	1801(6)	485(27)
C(11)	4856(4)	1357(5)	4312(7)	615(32)					

^{a} Equivalent isotropic U defined as one-third of the trace of the orthogonalized $\mathbf{U}_{ij}$ tensor.
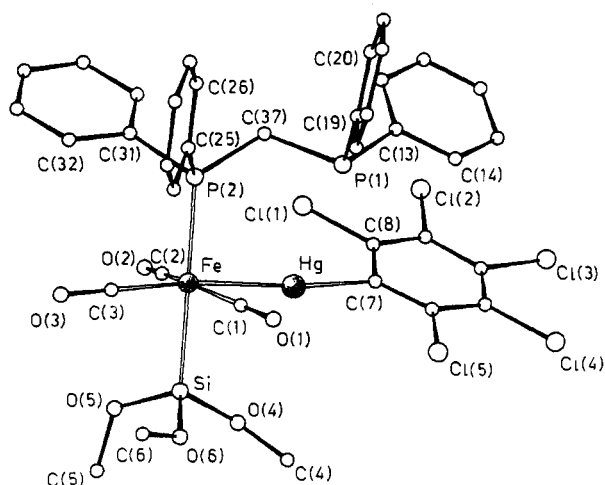
Figure 1. Molecular structure of [(OC)$_3${(MeO)$_3$Si}Fe(μ-dppm)Hg(C$_6$Cl$_5$)] (2).

Results

Complex mer-[(OC)$_3${(MeO)$_3$Si}Fe(μ-dppm)Hg(C$_6$Cl$_5$)] (2) has been previously obtained by the reaction of K[Fe{Si(OMe)$_3$}(CO)$_3$(dppm-*P*)] (1) with [HgCl(C$_6$Cl$_5$)].[3f] Although the ^{31}P{^{1}H} and ^{199}Hg{^{1}H} NMR data (δ −584, ^{2+3}J(Hg−P) = 242, ^1J(Hg−P) = 558 Hz) clearly indicate a significant ^1J(P−Hg) coupling, the solid-state structure of 2 (Figure 1), which has now been determined, reveals a rather long Hg−P distance (see below). The variation of ^1J(Hg−P) as a function of the substituent on Hg has been noted[3f] and could reflect changes of the spatial proximity between these two nuclei in the "average" solution structure. Differences between molecular structures in solution and in the solid state often indicate a shallow energy minimum for the latter. The dashed arrow from P to Hg used in the drawing of 2 (likewise for the O to Hg bond in 3 and 4) indicates what we believe to be weak bonding interactions, including

those of the van der Waals type. Reaction of 2 with 1 equiv of [Pt(C$_2$H$_4$)(PPh$_3$)$_2$] afforded two isomeric complexes in a 1:1 ratio, as deduced from the ^{31}P{^{1}H} NMR spectrum of the reaction mixture. Isomers cis-[(OC)$_3$Fe{μ-Si(OMe)$_2$(OMe)}(μ-dppm)(μ-Hg)Pt(C$_6$Cl$_5$(PPh$_3$)] (3) and trans-[(OC)$_3$Fe{μ-Si(OMe)$_2$(OMe)}(μ-dppm)(μ-Hg)-Pt(C$_6$Cl$_5$)(PPh$_3$)] (4) differ by the position of the PPh$_3$ ligand with respect to the Pt-bound dppm phosphorus atoms. Insertion of Pt(0) into the Hg−C bond of 2 has formally occurred, followed by loss of PPh$_3$ (eq 4).
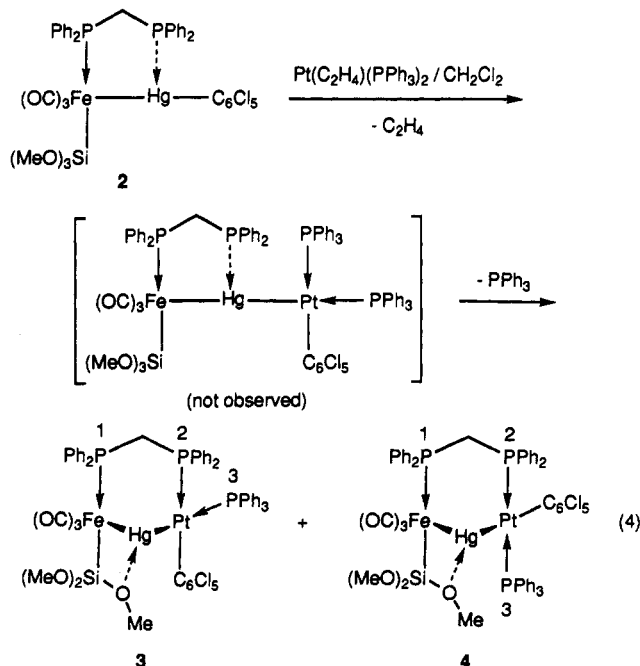

Interestingly, the bright yellow microcrystalline complex 3 was independently obtained in high yield in the

Table 3. Fractional Atomic Coordinates ($\times 10^4$) and Equivalent Isotropic Thermal Parameters ($\text{Å}^2 \times 10^4$) with Esd's in Parentheses for the Non-Hydrogen Atoms of [{(MeO)$_3$Si)}(OC)$_3$Fe(μ-dppm)HgPt(C$_6$Cl$_5$)(t-BuNC)(PPh$_3$)] (7·CH$_2$Cl$_2$)

	x/a	y/b	z/c	$U_{eq}{}^a$		x/a	y/b	z/c	$U_{eq}{}^a$
Pt	1559(1)	1298(1)	3037(1)	427(8)	C(23)	3548(27)	569(13)	2785(21)	783(118)
Hg	−474(1)	1256(1)	2468(1)	479(9)	C(24)	4016(21)	1849(10)	3427(17)	395(86)
Fe	−2424(4)	1137(2)	2268(3)	449(25)	C(25)	4403(26)	1781(13)	2865(21)	921(129)
Si	−1811(9)	763(4)	3482(7)	554(62)	C(26)	4849(25)	2159(14)	2682(20)	974(141)
P(1)	3350(7)	1320(4)	3647(5)	478(49)	C(27)	4785(24)	2639(13)	2968(19)	822(120)
P(2)	−3051(7)	1460(3)	1068(5)	478(49)	C(28)	4330(22)	2717(11)	3436(18)	669(101)
P(3)	−1583(7)	963(3)	556(5)	580(51)	C(29)	3893(23)	2300(11)	3669(17)	605(100)
Cl(1)	1083(7)	2332(3)	3793(5)	679(54)	C(30)	3967(22)	1384(10)	4733(15)	387(84)
Cl(2)	1078(7)	3419(3)	3217(5)	928(60)	C(31)	5016(23)	1509(9)	5156(18)	491(91)
Cl(3)	1485(8)	3600(3)	1793(6)	1065(66)	C(32)	5523(25)	1557(10)	5952(19)	688(105)
Cl(4)	1735(9)	2696(4)	876(6)	1121(74)	C(33)	4792(26)	1480(11)	6284(20)	877(120)
Cl(5)	1720(7)	1616(3)	1453(5)	717(56)	C(34)	3772(24)	1349(11)	5913(17)	673(95)
O(1)	−1807(19)	192(9)	1910(14)	923(157)	C(35)	3410(22)	1288(12)	5097(16)	591(82)
O(2)	−4505(16)	901(8)	2038(11)	670(129)	C(36)	−4452(22)	1616(10)	633(16)	365(83)
O(3)	−1941(23)	2043(9)	3197(15)	1206(206)	C(37)	−5242(25)	1299(14)	124(17)	716(102)
O(4)	−2157(19)	1035(8)	4092(12)	766(139)	C(38)	−6360(24)	1408(11)	−131(16)	608(100)
O(5)	−518(18)	702(8)	3996(13)	781(141)	C(39)	−6546(28)	1846(12)	128(19)	757(112)
O(6)	−2278(16)	197(8)	3345(11)	755(136)	C(40)	−5787(25)	2166(11)	578(18)	665(105)
N	1526(20)	195(9)	3499(16)	693(166)	C(41)	−4723(25)	2035(11)	862(18)	596(104)
C(1)	−2005(25)	578(12)	2116(19)	549(107)	C(42)	−2541(24)	2035(11)	885(20)	617(97)
C(2)	−3613(24)	984(10)	2142(16)	415(87)	C(43)	−1685(28)	2327(14)	1480(23)	915(138)
C(3)	−2058(29)	1685(14)	2842(23)	853(133)	C(44)	−1371(27)	2771(14)	1252(23)	953(133)
C(4)	1487(25)	600(12)	3372(19)	634(106)	C(45)	−1772(26)	2909(13)	500(22)	810(117)
C(5)	1365(20)	2006(9)	2564(17)	365(76)	C(46)	−2541(26)	2635(14)	−46(22)	972(135)
C(6)	1239(24)	2413(13)	2978(22)	853(123)	C(47)	−2940(26)	2212(13)	138(22)	928(126)
C(7)	1342(23)	2951(12)	2756(18)	600(100)	C(48)	−2962(22)	1004(10)	374(16)	545(102)
C(8)	1463(21)	2996(11)	2097(18)	531(89)	C(49)	−1513(26)	270(11)	339(18)	546(91)
C(9)	1580(19)	2592(10)	1715(16)	396(80)	C(50)	−522(30)	75(14)	720(21)	921(131)
C(10)	1572(22)	2128(11)	1963(17)	434(87)	C(51)	−389(35)	−436(16)	610(23)	1203(159)
C(11)	1448(29)	−349(13)	3641(22)	769(119)	C(52)	−1203(32)	−663(14)	131(21)	952(130)
C(12)	544(27)	−435(13)	3811(21)	873(126)	C(53)	−2257(37)	−501(18)	−244(25)	1448(179)
C(13)	2524(31)	−553(16)	4006(26)	1445(189)	C(54)	−2372(28)	8(14)	−140(19)	837(123)
C(14)	1030(36)	−540(16)	2724(26)	1941(234)	C(55)	−1613(21)	1258(12)	−316(16)	496(77)
C(15)	−3199(32)	1119(16)	3909(21)	1255(171)	C(56)	−2376(25)	1105(11)	−1062(19)	829(118)
C(16)	108(26)	1079(12)	4504(18)	728(122)	C(57)	−2342(27)	1348(16)	−1734(21)	985(129)
C(17)	−2009(27)	−151(12)	3961(22)	933(131)	C(58)	−1592(31)	1705(14)	−1539(25)	1130(148)
C(18)	3891(24)	767(11)	3482(20)	500(98)	C(59)	−951(30)	1888(15)	−853(24)	1096(148)
C(19)	4650(26)	446(13)	4100(22)	914(129)	C(60)	−965(25)	1648(12)	−216(21)	830(118)
C(20)	5076(28)	3(14)	3909(22)	935(129)	Cl(6)	4528(9)	4078(4)	3082(6)	1254(40)
C(21)	4618(32)	−145(15)	3140(26)	1252(161)	Cl(7)	4497(10)	4886(4)	4038(7)	1384(45)
C(22)	3853(24)	128(12)	2539(20)	693(113)	C(61)	3704(43)	4539(17)	3113(28)	1844(234)

^{a} Equivalent isotropic U defined as one-third of the trace of the orthogonalized U_{ij} tensor.

instantaneous reaction of **1** with *trans*-[PtCl{Hg(C$_6$-Cl$_5$)}(PPh$_3$)$_2$] (eq 5). This reaction did not follow the
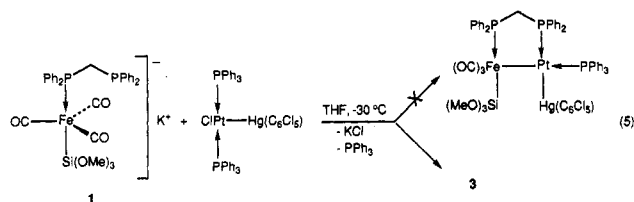
course expected on the basis of eq 3 which should have resulted in a complex with a Fe—Pt—Hg metal sequence. Complex **3** can be stored in air for prolonged periods of time but decomposes slowly in solution with precipitation of elemental mercury. The IR spectrum shows, in THF, the three characteristic ν(CO) absorptions of a meridional arrangement of terminal CO ligands around the iron center at 1991, 1936, and 1918 cm^{-1}. Three resonances are observed in the ^{31}P{^{1}H} NMR spectrum (Figure 2), a doublet at δ 52.9 for the iron-bound P^1 with a ^{2+4}J(P^1—P^2) coupling of 8 Hz, a doublet at δ 38.2 corresponding to P^3 with a ^2J(P^2—P^3) coupling of 11 Hz, and a doublet of doublets at δ 9.9 corresponding to P^2. (Note that the labeling of the P nuclei used in the NMR discussion is that given in the equations, not in the figures of the X-ray structures.) The latter two phos-

phorus atoms display additional ^1J(P^3—^{195}Pt) and ^1J(P^2—^{195}Pt) couplings of 2818 and 2532 Hz, respectively, whereas for P^1 a ^3J(P^1—^{195}Pt) of only 20 Hz is found. A ^{31}P{^{1}H} NMR spectrum recorded at 161.98 MHz confirmed the values of the coupling constants derived from the spectrum recorded at 81.02 MHz. In the ^{31}P{^{1}H} NMR, ^{199}Hg satellites were observed for P^1 and P^2 of 317 and 551 Hz, respectively. A ddd pattern was observed in the ^{199}Hg{^{1}H} NMR spectrum at δ −308 with a large ^2J(Hg—P^3) coupling of 2867 Hz and ^2J(Hg—P^1) and ^2J(Hg—P^2) values of 308 and 547 Hz, respectively, similar to those found in the ^{31}P{^{1}H} NMR spectrum (Table 5). In the ^{1}H NMR of **3** a triplet is found at δ 3.02 for the methylene group of the dppm ligand (^2J(H—P) = 10 Hz), which displays an additional ^3J(H—^{195}Pt) coupling of 40 Hz. A sharp singlet resonance for the Si(OMe)$_3$ group is observed at δ 3.42. The geometry of the molecule could not be established unambiguously from these data and will be further discussed below.

When a THF or toluene solution of **3** was stirred for 1 h at 70 °C, isomer **4** in which the phosphorus atoms are *trans* to each other was formed in almost quantitative yield. **4** forms orange crystals which are air-stable for a prolonged period of time. It is soluble in THF and chlorinated solvents and diethyl ether, whereas it is
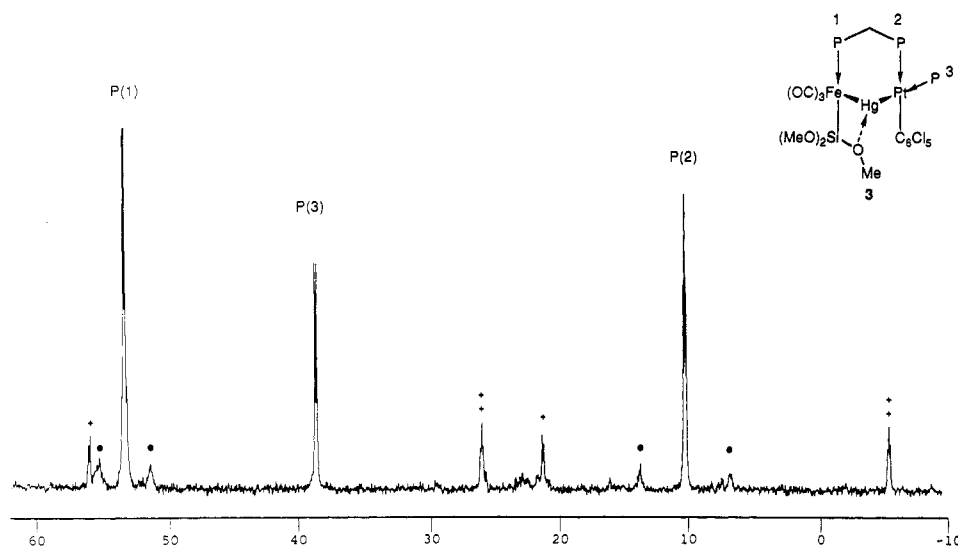
Figure 2. $^{31}P\{^1H\}$ NMR spectrum of cis-[(OC)$_3$Fe{μ-Si(OMe)$_2$(OMe)}(μ-dppm)(μ-Hg)Pt(C$_6$Cl$_5$)(PPh$_3$)] (3) in THF/C$_6$D$_6$. Platinum satellites are indicated by (+) and mercury satellites by (·).

Table 4. Fractional Atomic Coordinates ($\times 10^4$) and Equivalent Isotropic Thermal Parameters ($\text{Å}^2 \times 10^4$) with Esd's in Parentheses for the Non-Hydrogen Atoms of [{(MeO)$_3$Si)(OC)$_3$Fe(μ-dppm)(μ-SnCl$_2$)PtCl(PEt$_3$)] (10·CH$_2$Cl$_2$)

	x/a	y/b	z/c	U_{eq}^a		x/a	y/b	z/c	U_{eq}^a
Pt	2193(1)	1844(1)	172(1)	402(1)	C(14)	2506(4)	4564(5)	−206(5)	514(22)
Sn	1446(1)	1664(1)	1916(1)	427(1)	C(15)	1720(4)	5208(7)	−343(7)	699(31)
Fe	2280(1)	961(1)	3689(1)	398(3)	C(16)	1497(6)	6242(8)	−1225(10)	994(46)
Cl(1)	3066(1)	1909(2)	−1303(1)	604(7)	C(17)	2040(7)	6554(8)	−1876(8)	1000(50)
Cl(2)	527(1)	3725(2)	1905(2)	664(7)	C(18)	2813(6)	5934(8)	−1720(7)	837(38)
Cl(3)	367(1)	816(2)	2056(2)	631(7)	C(19)	3047(5)	4941(7)	−885(6)	672(29)
P(1)	2777(1)	3141(1)	819(1)	409(5)	C(20)	3843(3)	2606(5)	956(5)	439(19)
P(2)	2618(1)	2739(1)	3412(1)	402(5)	C(21)	4244(4)	1391(6)	887(5)	530(23)
P(3)	1519(1)	850(2)	−693(1)	481(6)	C(22)	5057(4)	960(8)	1025(7)	748(32)
Si	2076(1)	−982(2)	4059(2)	597(8)	C(23)	5456(5)	1757(10)	1214(8)	892(42)
O(1)	3448(3)	−485(4)	2351(4)	655(20)	C(24)	5064(5)	2959(10)	1243(8)	875(43)
O(2)	3094(3)	186(5)	5802(4)	667(21)	C(25)	4244(4)	3417(7)	1148(7)	634(28)
O(3)	763(3)	2035(5)	4622(5)	749(23)	C(26)	3639(3)	2574(5)	3703(5)	456(20)
O(4)	1935(3)	−1429(4)	2936(4)	630(20)	C(27)	4216(3)	1435(6)	3776(6)	535(23)
O(5)	2890(4)	−1978(5)	4651(6)	1018(33)	C(28)	4996(4)	1325(7)	3981(7)	681(29)
O(6)	1502(5)	−1188(10)	4989(6)	1672(62)	C(29)	5193(5)	2382(9)	4097(8)	814(39)
C(1)	3000(4)	88(5)	2859(5)	483(21)	C(30)	4648(5)	3476(9)	4046(7)	800(39)
C(2)	2794(4)	469(6)	4972(6)	499(23)	C(31)	3856(4)	3627(7)	3828(7)	625(28)
C(3)	1344(3)	1611(6)	4247(6)	528(24)	C(32)	2095(3)	3755(5)	4359(5)	448(20)
C(4)	1621(9)	−2407(11)	2854(8)	1219(66)	C(33)	2372(5)	3524(7)	5410(6)	673(30)
C(5)	3136(9)	−3257(10)	4868(14)	1504(80)	C(34)	1937(5)	4190(8)	6194(7)	746(36)
C(6)	777(7)	−1267(16)	5024(13)	1889(106)	C(35)	1227(6)	5054(8)	5896(7)	776(37)
C(7)	2443(3)	3792(5)	2081(5)	413(18)	C(36)	933(4)	5287(7)	4852(7)	694(31)
C(8)	1600(4)	−725(6)	−54(6)	581(27)	C(37)	1371(4)	4647(6)	4078(6)	550(24)
C(9)	2443(5)	−1571(8)	113(8)	844(38)	C(38)	4888(7)	2558(11)	8043(10)	1185(35)
C(10)	1820(5)	715(8)	−2074(6)	696(34)	Cl(4)	5355(3)	3642(5)	8201(5)	2171(21)
C(11)	1335(7)	223(11)	−2742(8)	993(53)	Cl(5)	4723(5)	2305(8)	6778(7)	1626(28)
C(12)	461(4)	1649(7)	−826(7)	690(31)	Cl(5')	4378(7)	3662(11)	6840(9)	2188(42)
C(13)	255(7)	3011(9)	−1378(12)	1277(64)					

^{a} Equivalent isotropic U defined as one-third of the trace of the orthogonalized U_{ij} tensor.

Table 5. $^{31}P\{^1H\}$ and $^{199}Hg\{^1H\}$ NMR Data for Complexes 3 and 4

	$^{31}P\{^1H\}$ NMR										$^{199}Hg\{^1H\}$ NMR			
	δ			J(P–P)/Hz			J(P–^{195}Pt)/Hz				$J(^{199}$Hg–P)/Hz			
	P^1	P^2	P^3	$^2J(P^1-P^2)$	$^4J(P^1-P^3)$	$^2J(P^2-P^3)$	$^3J(P^1-Pt)$	$^1J(P^2-Pt)$	$^1J(P^3-Pt)$	δ^c	$^2J(P^1-Hg)$	$^2J(P^2-Hg)$	$^2J(P^3-Hg)$
3^a	52.9	9.9	38.2	8		11	20	2532	2818	−308	308	547	2867
4^{a,b}	57.2	18.6	26.9	10.6	−0.8	391.0	9	2907	3200	−83	215	547	215

^{a} In CH$_2$Cl$_2$/C$_6$D$_6$. ^{b} Determined by spectral simulation. ^{c} Relative to HgMe$_2$, downfield chemical shifts reported as positive.

scarcely soluble in hexane. In solution 4 slowly decomposes with precipitation of elemental mercury. In THF, three IR absorptions characteristic of a *mer* arrangement of the carbonyl groups around the iron atom were observed at 1985, 1926, and 1906 cm^{-1}, ca. 10 cm^{-1} lower than those for 3. In the $^{31}P\{^1H\}$ NMR of 4, two characteristic sets of resonances due to an ABX spin system are observed, the X-part formed by the iron-bound phosphorus atom displaying a doublet resonance at δ 57.2 and the characteristic multiplet of the AB part consisting of two chemically inequivalent phosphorus atoms situated at δ 26.9 (P^3) and 18.6 (P^2) (Figure 3).
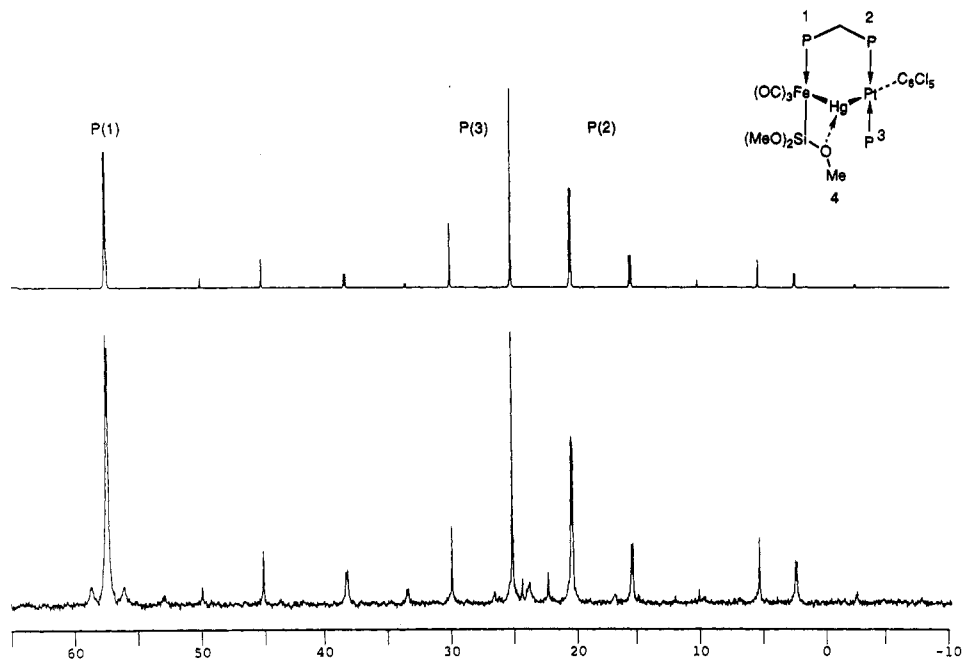
Figure 3. $^{31}P\{^1H\}$ NMR spectrum of *trans*-[(OC)₃Fe{μ-Si(OMe)₂(OMe)}(μ-dppm)(μ-Hg)Pt(C₆Cl₅)(PPh₃)] (4): (bottom) in THF/C₆D₆ at 293 K; (top) simulation (PANIC Bruker) of the ABX spin system (^{199}Hg satellites omitted).

The J(P−P) coupling constants and chemical shift values were calculated by spectral simulation. The P¹ iron-bound phosphorus atom is coupled to the platinum-bound phosphorus atoms P² (dppm) and P³ (PPh₃) by +10.6 and −0.8 Hz, respectively. The P² and P³ atoms are coupled with a ^2J(P²−P³) of 391.0 Hz, indicating a mutual *trans* position. ^1J(P−^{195}Pt) couplings of 3200 and 2907 Hz are found for the P³ and P² phosphorus atoms, respectively, whereas for P¹ a ^3J(P¹−^{195}Pt) coupling of only 9 Hz was observed. Significant J(P−^{199}Hg) couplings are found for all three phosphorus resonances, and the ^{199}Hg{¹H} NMR spectrum contained a doublet of triplets at δ −83 with ^2J(P−Hg) couplings of 215 (P¹ and P³) and 547 Hz (P²), which are identical with the couplings found in the $^{31}P\{^1H\}$ NMR spectrum. An additional ^1J(^{199}Hg−^{195}Pt) of 6320 Hz was evidenced. In the ¹H NMR spectrum, the resonance of the methylene group from the dppm ligand is found as a dt at δ 3.17, and displays additional ^3J(H−^{195}Pt) satellites of ca. 45 Hz. The sharp singlet resonance at δ 3.49 is due to the Si(OMe)₃ protons. The geometry of 4 is discussed below.

It is known that alkoxysilyl groups can be fluorinated under mild conditions by reaction with BF₃.[10] We synthesized recently [(OC)₃(F₃Si)Fe(μ-dppm)PtH(PPh₃)] by reaction of excess BF₃ with [(OC)₃{(MeO)₃Si}Fe(μ-dppm)PtH(PPh₃)] (5).[3g] However, reaction of 3 with 1 equiv of BF₃ yielded, upon immediate precipitation of elemental mercury, the cationic complex [(OC)₃Fe{μ-Si(OMe)₂(OMe)}(μ-dppm)Pt(PPh₃)]⁺ [11] in almost quantitative $^{31}P\{^1H\}$ NMR spectroscopic yields (by comparison

with an authentic sample), probably with [BF₃(C₆Cl₅)]⁻ as the counterion (eq 6).
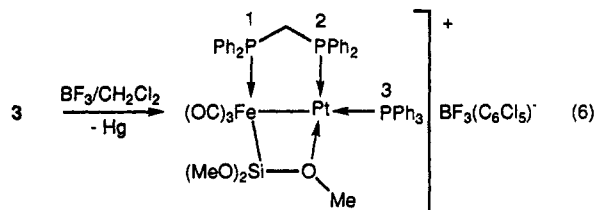
Considering the isolobal analogy between H⁺ and HgR⁺, we attempted the synthesis of the Fe−Pt−Hg complex shown in eq 7 by reacting a cold solution of 5 with a solution of [Hg(C₆Cl₅)]PF₆, prepared by stirring
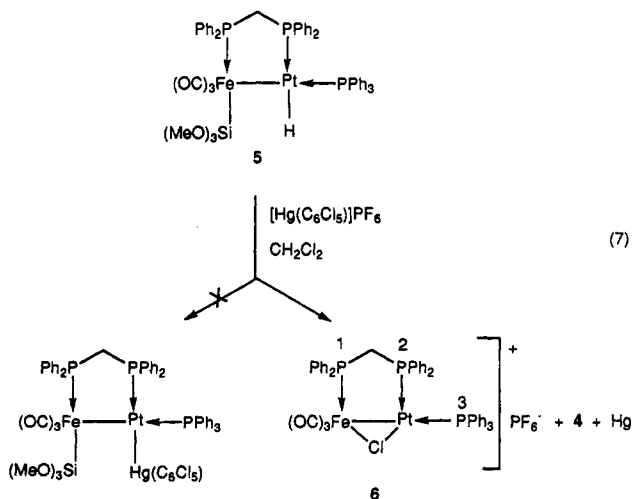
TlPF₆ and [HgCl(C₆Cl₅)] for 24 h in CH₂Cl₂. On warming to room temperature, the color of the solution changed from yellow to red and precipitation of elemental mercury was observed. $^{31}P\{^1H\}$ NMR spectroscopy of the reaction mixture indicated the formation of

(10) (a) Colomer, E.; Corriu, R. J. P.; Vioux, A. *Inorg. Chem.* **1979**, *18*, 695. (b) Marks, T. J.; Seyam, A. M. *Inorg. Chem.* **1974**, *13*, 1624.
(11) Knorr, M.; Braunstein, P. Unpublished results.

[(OC)₃Fe(μ-dppm)(μ-Cl)Pt(PPh₃)]PF₆ (**6**) and of some **4** (eq 7). Complex **4** was not observed when a solution of **5** was added to a solution of [Hg(C₆Cl₅)]⁺ (see Experimental Section). Red, air-stable crystals of **6** were characterized by the usual analytical and spectroscopic methods. In the FAB⁺ mass spectrum the molecular peak with its characteristic isotopic pattern was detected at *m/e* 1016.6. The relatively high IR absorptions at 2055, 2007, and 1986 cm⁻¹ in CH₂Cl₂ are consistent with a cationic species having carbonyls in a *mer* arrangement around the iron atom. The ¹H NMR spectrum showed no resonance for the Si(OMe)₃ protons, indicating the loss of this ligand. A triplet resonance was observed for the dppm protons, displaying platinum satellites with a ³J(H–Pt) coupling of 61 Hz. The ³¹P-{¹H} NMR spectrum showed four characteristic multiplet resonances, including that of the PF₆ anion. At δ 64.6 a doublet of doublets is found for the iron-bound phosphorus atom, with a ³⁺⁴J(P¹–P³) coupling of 37 Hz and an additional ²⁺³J(P¹–P²) coupling of 20 Hz. The doublet of doublets resonance at δ 30.6 represents the PPh₃ phosphorus atom with a ²J(P–P) coupling of 18 Hz and a ¹J(P–¹⁹⁵Pt) of 2970 Hz, and the triplet resonance is found at δ 2.2 with ¹J(P²–¹⁹⁵Pt) of 4717 Hz. The origin of the bridging chlorine atom is unclear, the solvent CH₂Cl₂ or the pentachlorophenyl ligand could both serve as chlorine sources. A complex formulated as [(OC)₃Fe(μ-dppm)(μ-I)PtI(PPh₃)] was recently identified by ³¹P{¹H} NMR spectroscopy but could not be isolated owing to its instability.[12] Its reported spectroscopic data are similar to those observed for **6**.

Solutions of **3** in toluene react with isonitriles or CO to give in almost quantitative yields the new complexes [(OC)₃{(MeO)₃Si}Fe(μ-dppm)HgPt(C₆Cl₅)(L)(PPh₃)] [L = *t*-BuNC (**7**), (2,6-xylyl)NC (**8**), CO (**9**)] (eq 8). They form

$$3 \xrightarrow{\text{L / CH}_2\text{Cl}_2}$$

7	L = (*t*-Bu)NC
8	L = (2,6-Xylyl)NC
9	L = CO
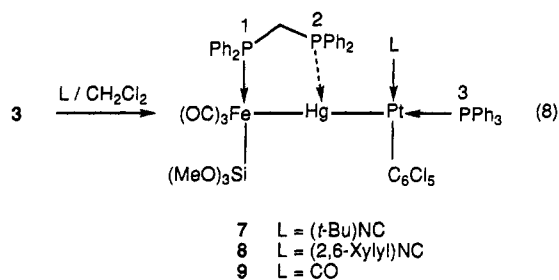
yellow microcrystalline powders which can be stored under N₂ for prolonged periods of time. In solution, slow decomposition with elimination of elemental Hg is observed. Complexes **7**–**9** were characterized by spectroscopic and analytical methods, and the structure of **7** was determined by a single-crystal X-ray diffraction study (Figure 4), which will be discussed below. The typical IR spectrum for three carbonyls in a *mer* arrangement was observed in all three cases. In their ³¹P{¹H} NMR spectra (Table 6, Figure 5) three characteristic resonances are detected between δ 53.3 and 54.7 (dd) for the iron-bound P¹ phosphorus atom of dppm, between δ 28.7 and 36.5 (dd) for the platinum-bound
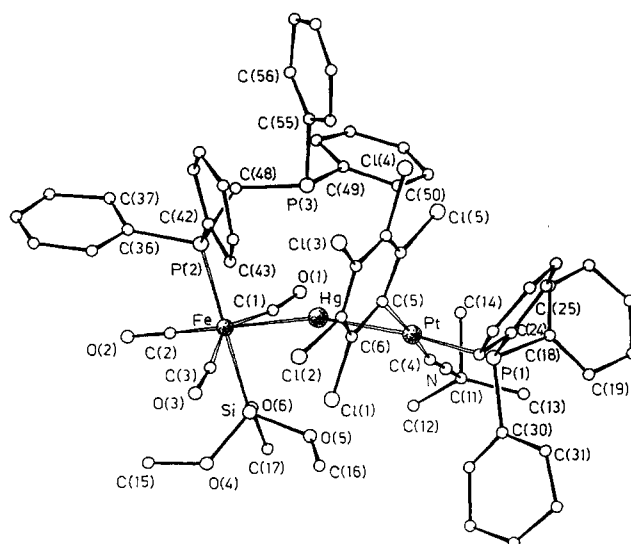
(12) Jacobsen, G. B.; Shaw, B. L.; Thornton-Pett, M. *J. Chem. Soc., Dalton Trans.* **1987**, 3079.

Figure 4. Molecular structure of *mer*-[(OC)₃{(MeO)₃Si}-Fe(dppm)HgPt(C₆Cl₅)(*t*-BuNC)(PPh₃)] as **7**·CH₂Cl₂.

phosphorus P³, and between δ −25.3 and −27.5 (dd) for the second phosphorus atom P² of the dppm ligand. All resonances display platinum and mercury satellites (see Discussion), and for **7** these coupling constants were also determined by ¹⁹⁹Hg{¹H} NMR spectroscopy, where a ddd resonance was found at δ −753. The chemical shift values found in the ¹⁹⁹Hg{¹H} NMR spectrum of complexes of the type [(OC)₃{(MeO)₃Si}Fe(μ-dppm)HgR] (R = C₆Cl₅ (**2**), δ −584; R = Pt(C₆Cl₅)(*t*-BuNC)(PPh₃) (**7**), δ −753; R = Fe{Si(OMe)₃}(CO)₃(dppm-*P*),³ᵏ δ −658) are substantially shifted to a higher field when compared to the values of **3** (δ −308) and **4** (δ −83).

When a solution of 1 equiv of K[Fe{Si(OMe)₃}(CO)₃-(dppm-*P*)] was added at a low temperature to a solution of *trans*-[PtCl(SnCl₃)(PEt₃)₂], the cyclic, stannylene-bridged complex [(OC)₃{(MeO)₃Si}Fe(μ-dppm)(μ-SnCl₂)-PtCl(PEt₃)] (**10**) was formed in high yields (eq 9). **10**

10
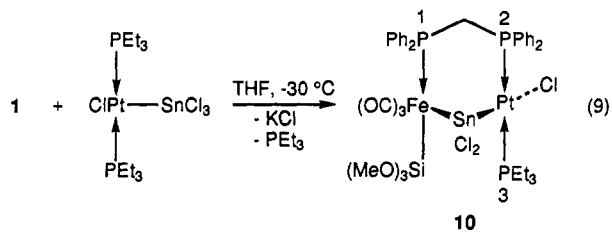
forms yellow crystals, which can be stored at 0 °C under nitrogen for prolonged periods of time. Solutions of **10** are stable at low temperature but decompose rapidly at room temperature. Single crystals suitable for X-ray diffraction were obtained by slow diffusion of hexane into a CH₂Cl₂ solution (Figure 6) (see below). The FAB⁺ mass spectrum contains a peak at *m/e* 1148.7, corresponding to (M⁺ − Cl) with a characteristic isotopic pattern. Fragments corresponding to the loss of CO, Cl, and Si(OMe)₃ groups were also detected (see Experimental Section). The IR spectrum of **10** in THF shows three characteristic absorptions at 2037, 1985, and 1967 cm⁻¹, indicating a *mer* arrangement of the iron-bound carbonyl groups. The presence of the Si-

Table 6. $^{31}P\{^1H\}$ NMR Data for Complexes 7–9 and $^{199}Hg\{^1H\}$ NMR Data for 7

| | $^{31}P\{^1H\}$ NMR[d] | | | | | | | | | $^{199}Hg\{^1H\}$ NMR | | | |
| | δ | | | J(P–P)/Hz | | | J(P–^{195}Pt)/Hz | | | | J(P–^{199}Hg)/Hz | | |
	P^1	P^2	P^3	^2J(P^1–P^2)	^3J(P^2–P^3)	^4J(P^1–P^3)	^3J(P^1–Pt)	^2J(P^2–Pt)	^1J(P^3–Pt)	δ^c	^2J(P^1–Hg)	^1J(P^2–Hg)	^2J(P^3–Hg)
7^a	54.5	−25.4	28.7	96	7.2	5.7	35	35	2350	−753	100	215	3000
8^b	54.7	−27.5	30.5	93	6	6	35	35	2370		100	170	2830
9^b	53.3	−25.3	36.5	101	6	5	34	43	2213		75	270	

^{a} In THF/toluene-d_8. ^{b} In CH$_2$Cl$_2$/C$_6$D$_6$. ^{c} Relative to HgMe$_2$, downfield chemical shifts reported as positive. ^{d} The labeling of the P atoms is that given by eq 8, not Figure 4.
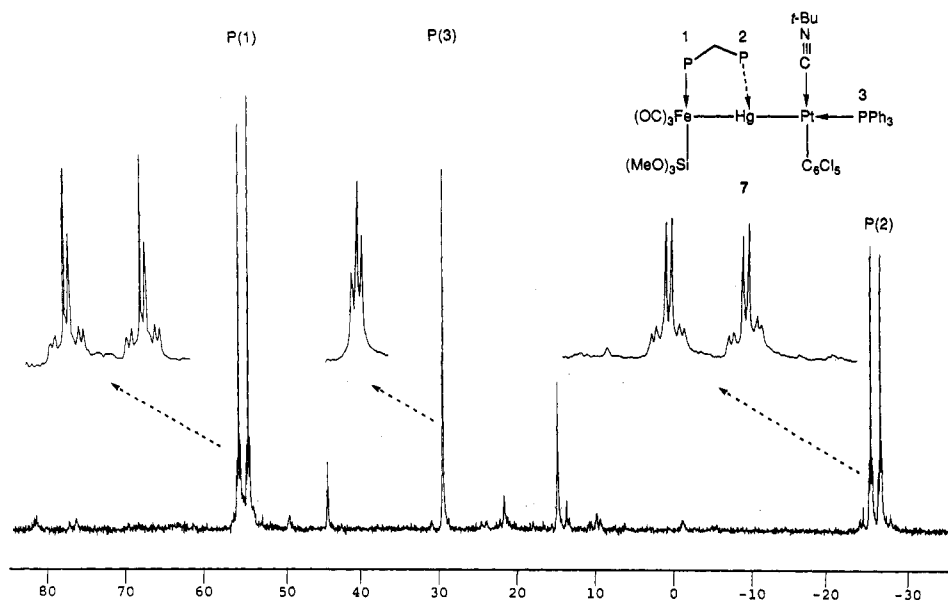
Figure 5. $^{31}P\{^1H\}$ NMR spectrum of *mer*-[(OC)$_3${(MeO)$_3$Si}Fe(dppm)HgPt(C$_6$Cl$_5$)(t-BuNC)(PPh$_3$)] (**7**) in CH$_2$Cl$_2$/C$_6$D$_6$.

(OMe)$_3$ group was evidenced by ^{1}H NMR spectroscopy as a sharp singlet resonance at δ 3.70. The $^{31}P\{^1H\}$ NMR was recorded at 263 K (Figure 7) and displays an ABX pattern with δ 37.0 for the iron-bound phosphorus atom and δ 15.2 and 11.0 for the platinum-bound phosphorus atoms P^3 and P^2, respectively. The J(P–P)́ coupling constants and chemical shift values were calculated by spectral simulation. The strong coupling of 366.8 Hz between P^2 and P^3 indicates their mutual *trans* position. All resonances display satellites due to couplings with the NMR-active ^{195}Pt (33.7%) and the ^{117,119}Sn isotopes (7.65 and 8.68% natural abundance, respectively). The ^2J(P–Sn) coupling constants are 200, 205, and 130 Hz for P^1, P^2, and P^3, respectively. The platinum-bound phosphorus atoms P^2 and P^3 display ^1J(P–Pt) coupling constants of 2316 and 2640 Hz, which are in the range found for complexes *trans*-[PtX$_2$-(PR$_3$)$_2$].[13,14] As expected, P^1 displays only a weak ^3J(P–^{195}Pt) coupling of 10 Hz.

When a deep red CH$_2$Cl$_2$ solution of *mer*-[(OC)$_3$Fe{μ-Si(OMe)$_2$(OMe)}(μ-dppmPdCl] was stirred with 1 equiv of SnCl$_2$, the new product *mer*-[(OC)$_3$Fe{μ-Si(OMe)$_2$-(OMe)}(μ-dppm)PdSnCl$_3$] (**11**) was formed in good yield and was characterized by spectroscopic and analytical

(13) Albinati, A.; von Gunten, U.; Pregosin, P. S.; Ruegg, H. J. *J. Organomet. Chem.* **1985**, *295*, 239.
(14) Pregosin, P. S. In *Phosphorus-31 NMR Spectroscopy in Stereochemical Analysis*; VCH Publishers: Weinheim, 1987; p 465.
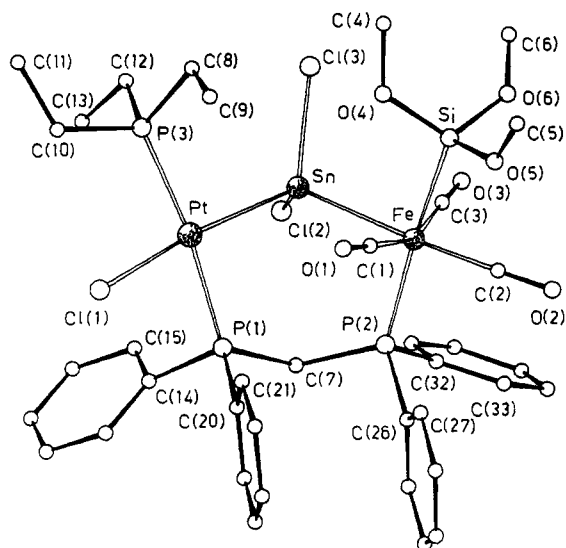
methods (eq 10). Red microcrystalline **11** is stable and
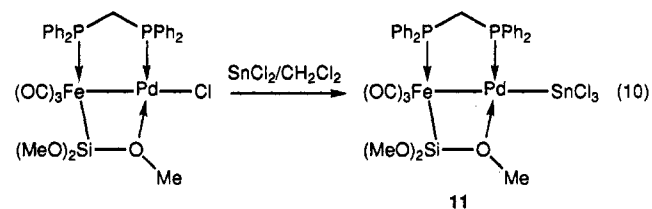
can be stored under nitrogen for prolonged periods of time. Absorptions were observed in the FIR spectrum at 321 (vs), 308 (s), and 307 (s) cm^{-1}, which appear typical for the −SnCl$_3$ ligand.[31b] The ^{1}H NMR spectrum of **11** displays a dd resonance for the methylene protons of the dppm ligand at δ 4.07 and a singlet resonance of the Si(OMe)$_3$ group at δ 3.81. At 193 K the latter signal splits up and gives rise to distinct resonances which could be due to the occurrence of a Fe–Si–O→Pd interaction, as observed in the −SnPh$_3$ derivative.[3c] In the $^{31}P\{^1H\}$ NMR spectrum two doublets at δ 43.8 and 30.6 for the iron- and palladium-bound phosphorus atoms, respectively, are detected, which display a ^{2+3}J(P–P) coupling constant of 52 Hz. However, no coupling with the ^{117,119}Sn isotopes could be evidenced, in contrast to the situation in the −SnPh$_3$ derivative, which may indicate an enhanced lability of the Cl$_3$Sn–Pd bond. In contrast to the formation of **11**, reaction of [(OC)$_3$Fe{μ-Si(OMe)$_2$(OMe)}(μ-dppm)PtCl]^{3a} with SnCl$_2$ did not lead to the expected insertion product containing a FePtSnCl$_3$ array; instead formation of various clusters

Figure 6. Molecular structure of [(OC)₃{(MeO)₃Si}Fe(μ-dppm)(μ-SnCl₂)PtCl(PEt₃)] as **10·CH₂Cl₂**.

was observed, inter alia with a PtFe₂ core (^{31}P NMR evidence and comparison with known spectra[3n]).

Description of the Crystal Structure of *mer*-

[(OC)₃{(MeO)₃Si}Fe(μ-dppm)Hg(C₆Cl₅)] (2). A view of the structure of **2** is shown in Figure 1; selected bond distances and angles are given in Table 7. The Fe and Hg centers are linked by a metal–metal bond [Fe–Hg = 2.528(3) Å]. The value of the Fe–Hg bond distance falls close to the shortest values, in the range 2.436–2.960 Å, reported for complexes containing Fe–Hg bonds (from Cambridge Crystallographic Data Centre) and is also much shorter than that found in **7** (see below). The distorted octahedral environment of the Fe atom is determined by the Hg atom, by three meridional carbon atoms from terminal carbonyl groups, by the P(2) atom from dppm [Fe–P(2) = 2.257(3) Å], and by a Si atom of the alkoxysilyl ligand [Fe–Si = 2.311(3) Å)] in apical positions. The Hg atom is bound also to a carbon atom, C(7), from the C₆Cl₅ ligand [Hg–C(7) = 2.117(7)

Table 7. Selected Bond Distances (Å) and Angles (deg) in Complex 2

Hg–Fe	2.528(3)	Si–O(4)	1.606(7)
Hg–C(7)	2.117(7)	Si–O(5)	1.644(7)
Fe–Si	2.311(3)	Si–O(6)	1.623(7)
Fe–P(2)	2.257(3)	C(1)–O(1)	1.134(11)
Fe–C(1)	1.785(9)	C(2)–O(2)	1.165(11)
Fe–C(2)	1.769(9)	C(3)–O(3)	1.134(9)
Fe–C(3)	1.770(7)	C(7)–C(8)	1.388(10)
C(8)–Cl(1)	1.733(8)	C(7)–C(12)	1.360(10)
C(9)–Cl(2)	1.729(9)	C(8)–C(9)	1.372(11)
C(10)–Cl(3)	1.723(9)	C(9)–C(10)	1.372(13)
C(11)–Cl(4)	1.729(9)	C(10)–C(11)	1.382(13)
C(12)–Cl(5)	1.724(8)	C(11)–C(12)	1.394(11)
Fe–Hg–C(7)	172.1(2)	Fe–C(1)–O(1)	178.4(8)
Hg–Fe–Si	87.4(1)	Fe–C(2)–O(2)	179.4(8)
Hg–Fe–P(2)	93.3(1)	Fe–C(3)–O(3)	177.9(6)
Hg–Fe–C(1)	79.6(3)	Hg–C(7)–C(8)	119.3(5)
Hg–Fe–C(2)	78.7(3)	Hg–C(7)–C(12)	123.5(5)
Si–Fe–C(1)	84.1(3)	C(8)–C(7)–C(12)	117.0(7)
Si–Fe–C(2)	86.5(3)	C(7)–C(8)–C(9)	122.4(7)
Si–Fe–C(3)	85.3(2)	C(8)–C(9)–C(10)	119.6(8)
P(2)–Fe–C(1)	96.0(3)	C(9)–C(10)–C(11)	119.5(8)
P(2)–Fe–C(2)	93.7(3)	C(10)–C(11)–C(12)	119.4(8)
P(2)–Fe–C(3)	94.1(2)	C(7)–C(12)–C(11)	122.0(7)
C(1)–Fe–C(3)	104.2(4)	P(1)–C(37)–P(2)	113.9(4)
C(2)–Fe–C(3)	96.2(4)		

Å], and the Fe–Hg–C(7) array is slightly bent [Fe–Hg–C(7) = 172.1(2)°]. The separation between the Hg atom and the P(1) atom from the dangling dppm [Hg,P(1) = 3.170(3) Å], appears too long for a significant bonding interaction, the mean value of the Hg–P bonds involving PPh₃ ligands being 2.453(34) Å (from Cambridge Crystallographic Data Centre). However, a conformer of **2** would have been conceivable in which the pendant phosphorus atom of the dppm ligand and the mercury atom would have been much further apart: a 180° rotation about the Fe-P(2) axis would have resulted in a situation similar to that found in Hg[Fe{Si(OMe)₃}-(CO)₃(dppm-*P*)]₂.[3k] We cannot state whether the orientation of the dppm ligand in **2** results from inter- or intramolecular effects. In contrast to the situation found in [Fe(CO)₃{μ-Si(OMe)₂(OMe)}(μ-dppm)PdCl] and
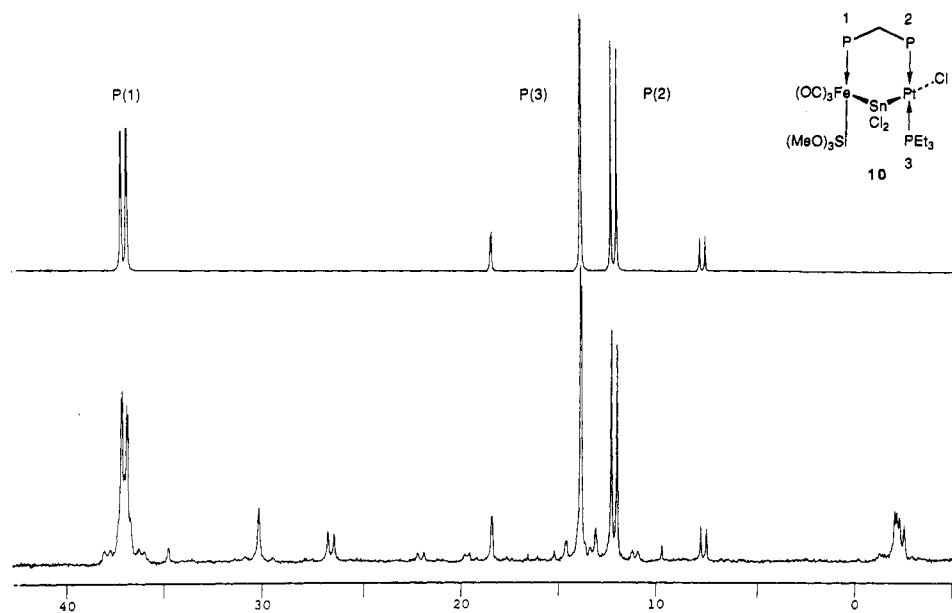

Figure 7. ^{31}P{^{1}H} NMR spectrum of [(OC)₃{(MeO)₃Si}Fe(μ-dppm)(μ-SnCl₂)PtCl(PEt₃)] (**10**): (bottom) in CH₂Cl₂/C₆D₆ at 263 K; (top) simulation (PANIC Bruker) of the ABX spin system ([195]Pt and [117/119]Sn satellites omitted).

Table 8. Selected Bond Distances (Å) and Angles (deg) in Complex 7·CH₂Cl₂

Hg–Pt	2.575(2)	Si–O(4)	1.64(3)
Hg–Fe	2.634(6)	Si–O(5)	1.64(2)
Pt–P(1)	2.257(9)	Si–O(6)	1.62(2)
Pt–C(4)	1.99(3)	N–C(4)	1.11(4)
Pt–C(5)	2.06(3)	N–C(11)	1.49(4)
Fe–Si	2.316(13)	C(1)–O(1)	1.19(4)
Fe–P(2)	2.236(10)	C(2)–O(2)	1.21(4)
Fe–C(1)	1.68(3)	C(3)–O(3)	1.14(5)
Fe–C(2)	1.64(3)	C(5)–C(6)	1.41(5)
Fe–C(3)	1.76(4)	C(5)–C(10)	1.36(5)
C(6)–Cl(1)	1.70(5)	C(6)–C(7)	1.53(5)
C(7)–Cl(2)	1.67(4)	C(7)–C(8)	1.37(5)
C(8)–Cl(3)	1.72(3)	C(8)–C(9)	1.36(4)
C(9)–Cl(4)	1.76(4)	C(9)–C(10)	1.33(4)
C(10)–Cl(5)	1.75(3)		
Fe–Hg–Pt	164.7(2)	C(1)–Fe–C(2)	100.1(17)
Hg–Pt–C(4)	83.2(11)	C(2)–Fe–C(3)	106.5(17)
Hg–Pt–C(5)	87.6(9)	C(14)–N–C(11)	174(3)
P(1)–Pt–C(4)	94.0(11)	Fe–C(1)–O(1)	171(3)
P(1)–Pt–C(5)	95.4(9)	Fe–C(2)–O(2)	176(3)
Hg–Fe–Si	91.5(4)	Fe–C(3)–O(3)	172(3)
Hg–Fe–P(2)	89.6(3)	Pt–C(4)–N	170(3)
Hg–Fe–C(1)	72.5(14)	Pt–C(5)–C(6)	119(2)
Hg–Fe–C(3)	79.8(15)	Pt–C(5)–C(10)	124(2)
Si–Fe–C(1)	78.2(11)	C(6)–C(5)–C(10)	116(3)
Si–Fe–C(2)	85.5(10)	C(5)–C(6)–C(7)	121(3)
Si–Fe–C(3)	81.9(13)	C(6)–C(7)–C(8)	114(3)
P(2)–Fe–C(1)	99.5(11)	C(7)–C(8)–C(9)	122(3)
P(2)–Fe–C(2)	93.1(10)	C(8)–C(9)–C(10)	121(3)
P(2)–Fe–C(3)	101.0(13)	C(5)–C(10)–C(9)	125(3)

Table 9. Selected Bond Distances (Å) and Angles (deg) in Complex 10·CH₂Cl₂

Pt–Sn	2.524(2)	Fe–C(1)	1.795(6)
Fe–Sn	2.568(2)	Fe–C(2)	1.782(7)
Pt–Cl(1)	2.379(2)	Fe–C(3)	1.785(6)
Pt–P(1)	2.316(2)	Si–O(4)	1.624(6)
Pt–P(3)	2.293(3)	Si–O(5)	1.649(6)
Sn–Cl(1)	2.427(3)	Si–O(6)	1.558(9)
Sn–Cl(2)	2.399(3)	C(1)–O(1)	1.125(8)
Fe–Si	2.326(3)	C(2)–O(2)	1.128(9)
Fe–P(2)	2.261(2)	C(3)–O(3)	1.129(8)
Sn–Pt–P(1)	90.4(1)	P(2)–Fe–C(3)	95.7(2)
Sn–Pt–P(3)	93.9(1)	C(1)–Fe–C(2)	99.9(3)
Cl(1)–Pt–P(1)	84.8(1)	C(2)–Fe–C(3)	94.9(3)
Cl(1)–Pt–P(3)	91.9(1)	Pt–Sn–Fe	115.8(1)
Sn–Fe–Si	93.9(1)	Pt–Sn–Cl(2)	105.2(1)
Sn–Fe–P(2)	91.5(1)	Pt–Sn–Cl(3)	121.4(1)
Sn–Fe–C(1)	83.4(2)	Fe–Sn–Cl(2)	109.6(1)
Sn–Fe–C(3)	81.2(2)	Fe–Sn–Cl(3)	111.0(1)
Si–Fe–C(1)	78.0(2)	Cl(2)–Sn–Cl(3)	89.6(1)
Si–Fe–C(2)	84.3(2)	Fe–C(1)–O(1)	178.3(6)
Si–Fe–C(3)	88.9(2)	Fe–C(2)–O(2)	177.3(7)
P(2)–Fe–C(1)	98.9(2)	Fe–C(3)–P(3)	177.9(6)
P(2)–Fe–C(2)	90.6(2)	P(1)–C(7)–P(2)	119.3(3)

in the Fe–Pt and Fe–Rh related complexes,[3a,d] there is no significant bonding interaction in **2** between the alkoxysilyl ligand and the Hg atom, the shortest contact between the Hg atom and an oxygen atom being 3.079-(8) Å with O(4).

Description of the Crystal Structure of *mer*-[(OC)₃{(MeO)₃Si}Fe(dppm)HgPt(C₆Cl₅)(*t*-BuNC)(P-Ph₃)] (7·CH₂Cl₂). In the crystals of **7** dichloromethane molecules of solvation are also present. A view of the structure of **7** is shown in the Figure 4; selected bond distances and angles are given in Table 8. The complex is characterized by a bent Fe–Hg–Pt chain [Fe–Hg–Pt = 164.7(2)°]. The coordination around Fe is very similar to that found in **2** and involves the Hg atom, three meridional carbon atoms from terminal carbonyl groups, the P(2) atom from dppm [Fe–P(2) = 2.236(10) Å], and a Si atom of the alkoxysilyl ligand [Fe–Si = 2.316(13) Å)]. The Pt atom is in a slightly distorted square planar arrangement, determined by the Hg atom, the C(5) atom from the C₆Cl₅ ligand [Pt–C(5) = 2.06(3) Å], the C(4) atom from the isocyanide ligand [Pt–C(4) = 1.99(3) Å], and the P(1) atom from the PPh₃ ligand [Pt–P(1) = 2.257(9) Å]. The Fe–Hg bond distance [2.634(6) Å] is much longer than that found in **2** and is a little longer than that in Hg[Fe{Si(OMe)₃}(CO)₃-(dppm-*P*)]₂ [2.574(1) Å].[3k] The value of the Hg–Pt bond distance [Hg–Pt = 2.575(2) Å] is comparable to that found in a W–Hg–Pt complex [2.572(1) Å][2a] and falls in the shortest range of values found in complexes with Hg–Pt bonds [2.510–3.084 Å, from cambridge Crystallographic Data Centre]. No bonding interaction is observed between the Hg atom and either the P(3) atom from the dangling dppm [Hg,P(3) = 3.369(9) Å] or the alkoxysilyl ligand, the shortest contact between the Hg atom and an oxygen atom of the latter ligand being 3.33-(3) Å with O(5). A semibridging character of a carbonyl might be envisaged, more by the relatively short Hg–

C(1) distance [2.66(3) Å] than by the bending of the Fe–C(1)–O(1) angle [171(3)°].

Description of the Crystal Structure of *mer*-[(OC)₃{(MeO)₃Si}Fe(μ-dppm)(μ-SnCl₂)PtCl(PEt₃)] (10·CH₂Cl₂). Dichloromethane molecules of solvation are also present in the crystals of **10**. A view of the structure is shown in the Figure 6; selected bond distances and angles are given in Table 9. The cyclic structure of **10** contains a bent Fe–Sn–Pt array [115.8-(1)°] whose terminal atoms are bridged by dppm. A somewhat related structural arrangement has been recently found in a Fe₂Au₂(μ-dppm)₂ cluster.[3k] The coordination around Fe is very similar to that found in **2** and **7** and involves the Sn atom, three meridional carbon atoms from terminal carbonyl groups, the P(2) atom from dppm [Fe–P(2) = 2.261(2) Å], and the Si atom of the alkoxysilyl ligand [Fe–Si = 2.326(3) Å)]. The Pt atom is in a slightly distorted square planar arrangement determined by the Sn atom, a terminal chlorine atom Cl(1) [Pt–Cl(1) = 2.379(2) Å], the P(3) atom from the PEt₃ ligand [Pt–P(3) = 2.293(3) Å], and the P(1) atom from the bridging dppm ligand [Pt–P(1) = 2.316(2) Å]. The Sn atom shows the expected tetrahedral coordination involving two chlorine atoms [Sn–Cl(2) = 2.427(3) and Sn–Cl(3) = 2.399(3) Å] and the two metals. The Pt–Sn bond distance [2.524(2) Å] falls in the shortest range of values found in complexes witn Pt–Sn bonds [2.470–2.974 Å, from Cambridge Crystallographic Data Centre]. The value of the Fe–Sn bond distance [2.568(2) Å] is very close to the mean value found in complexes in which Fe–Sn bonds were present [2.562 Å, from Cambridge Crystallographic Data Centre]. There is no significant bonding interaction between the alkoxysilyl ligand and the Sn atom, the shortest contact between the Sn atom and an oxygen atom being 3.390(5) Å with O(5).

Discussion

Formation and Geometry of the Fe–Hg–Pt Complexes 3 and 4. Insertion reactions of Pt⁰ fragments into transition metal carbon bonds are well documented, and in the reaction of eq 1, insertion selectively occurs in the Hg–C bond of the bimetallic R–Hg–m complex.[2a]

As a consequence, the reaction of $Pt(C_2H_4)(PPh_3)_2$ with 2 was expected to lead to a product similar to 7–9 with L = PPh_3 (eq 4). However, we observed the formation of 3 and 4 in a 1:1 ratio (by $^{31}P\{^1H\}$ NMR). Isomer 3 is selectively obtained, in high yields, by the reaction of eq 5 which does not lead to the isomeric array Fe–Pt–HgR, as would be anticipated from the reactions summarized in eq 3.

In complex 3 $^{31}P\{^1H\}$ NMR resonances can be unambiguously assigned to P^1, P^2, and P^3 by their mutual coupling constants (Table 5). The small $J(P^1-P^2)$ coupling constant of 8 Hz is consistent with values found in $M(\mu$-dppm)M' complexes which do not contain a metal–metal bond.[15] The small coupling of 11 Hz for $^2J(P^2-P^3)$ indicates a mutual *cis* arrangement of these two platinum-bound phosphorus atoms. The absence of a direct Fe–Pt bond could explain why no $J(P^1-P^3)$ was detected and why no considerable coupling of P^1 to ^{195}Pt was observed (keeping in mind, however, that no $^2J(P-^{195}Pt)$ was observed either in the metal–metal bonded *mer*-[(OC)$_3$Fe{μ-Si(OMe)$_2$(OMe)}(μ-dppm)PtCl]^{3a}). The iron- (P^1) and platinum-bound (P^2) phosphorus atoms of the dppm ligand display coupling constants with the NMR-active isotope ^{199}Hg (spin $^1/_2$, natural abundance 16.84%) whose values correspond to $^2J(P-^{199}Hg)$ couplings (Table 5). Phosphorus atoms of phosphine ligands bound to square planar transition metal centers in the *trans* position with respect to mercury atoms are known to display $^2J(P-^{199}Hg)$ couplings of several thousands of hertz.[16] The resonance of P^3 at δ 38.2 with its large $^2J(P-^{199}Hg)$ coupling constant of 2867 Hz therefore indicates its transoid position relative to the mercury atom. The large $^1J(^{195}Pt-^{199}Hg)$ coupling of ca. 11 000 Hz observed in the $^{199}Hg\{^1H\}$ NMR spectrum unambiguously indicates the presence of a Hg–Pt bond.

The $^{2+4}J(P-P)$ coupling constants in 3 or 4 are smaller than the $^{2+3}J(P-P)$ usually found in complexes containing a metal–metal bonded Fe(μ-dppm)Pt moiety (in the range 50–180 Hz).[3n,o] Examples of a mercury atom bridging a metal–metal bond are known for $HgCl_2$ and [XHg]$^+$ fragments.[17] A-frame complexes with μ_2-HgX units are rare. A structurally characterized example is [Rh$_2$(μ-pz)$_2$(μ-HgCl)Cl(CO)$_2$(PPh$_3$)$_2$] (pz = pyrazolate),[18] and a similar situation was also proposed in [Rh$_2$Cl$_3$(μ-HgCl)(CO)$_2$(μ-dppm)$_2$].[19] However no μ_2-bridging situation of a "naked" Hg atom has been structurally characterized so far, although a μ_3-Hg atom has been observed in a platinum cluster.[20]

In some structurally characterized examples of heterometallic Pt–Ag complexes containing platinum-bound C_6X_5 (X = F, Cl) ligands, their *ortho* halogen atoms show coordination to the adjacent metal centers and therefore stabilize the molecular geometry.[21] In the case of (NBu$_4$)[Sn{Pt(μ-Cl)(C$_6$F$_5$)$_2$}$_3$] a naked μ_3-Sn atom capping a platinum cluster was found and the *ortho* fluorine atoms of the C_6F_5 groups were believed to be responsible for the stability of this complex.[21c] Another example of the stabilizing effect of such ligands was observed in Pt–Hg–R (R = polychloroaryl) complexes which are stable toward demercuration reactions only if R bears chlorine atoms in the *ortho* position to the C–Hg bond.[2b,22] A comparable situation with a chlorine group stabilizing the bridging mercury atom could therefore be envisaged for 3 but obviously not for 4. This interaction would appear sterically more favorable than a bridging *ipso* carbon atom between Pt and Hg.
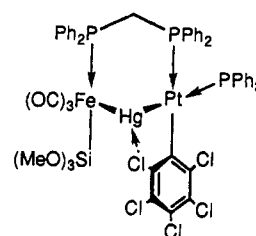
In a number of related bimetallic complexes containing the $Si(OMe)_3$ group we could show the presence of a four membered Fe–Si–O–M ring (M = Pt, Pd, Rh, Ag, Cd).[3] A chelating S–Si–O–Hg bridge has been reported for Hg[SSi(O-t-C$_4$H$_9$)$_3$]^{23} and a bridging interaction of the $Si(OMe)_3$ group to the Hg atom could therefore also be envisaged. Unfortunately, there is no evidence in the ^1H NMR spectrum for such an interaction where it should give rise to two distinct signals in a 2:1 ratio for the nine protons of the $Si(OMe)_3$ group. However, a rapid exchange of the OMe groups could also result in a singlet resonance for the methoxy protons, as observed in a Fe–Pd complex with a structurally characterized Fe–Si–O→Pd interaction.[3a]

The thermodynamically more stable isomer 4 is formed in a clean reaction upon heating a toluene solution of 3 for 30 min (Scheme 1). Formation of *mer*-[(OC)$_3$Fe{μ-Si(OMe)$_2$(OMe)}(μ-dppm)Pt(C$_6$Cl$_5$)] was not observed, which would be expected to be stable by analogy with *mer*-[(OC)$_3$Fe{μ-Si(OMe)$_2$(OMe)}(μ-dppm)Pt-Cl]. There are numerous examples of *cis/trans* isomerizations in square planar platinum complexes of the type $PtX_2(PR_3)_2$. The *trans* complexes are in general thermodynamically more stable than the *cis* isomers owing to the bond-weakening *trans* influence of the phosphine

(15) (a) Manojlovic-Muir, L.; Henderson, A. N.; Treurnicht, I.; Puddephatt, R. J.; *Organometallics* **1989**, *8*, 2055. (b) Braunstein, P.; Knorr, M.; Strampfer, M.; Dusausoy, Y.; Bayeul, D.; DeCian, A.; Fischer, J.; Zanello, P. *J. Chem. Soc., Dalton Trans.* **1994**, 1533.

(16) vanVliet, P. I.; Kuyper, J.; Vrieze, K. *J. Organomet. Chem.* **1976**, *122*, 99.

(17) (a) Sharp, P. R. *Inorg. Chem.* **1986**, *25*, 4185. (b) Braunstein, P.; Rosé, J.; Tiripicchio, A.; Tiripicchio-Camellini, M. *J. Chem. Soc., Dalton Trans.* **1992**, 911 and references cited. (c) Gade, L. *Angew. Chem., Int. Ed. Engl.* **1993**, *32*, 24 and references cited.

(18) Tiripicchio, A.; Lahoz, F. J.; Oro, L. A.; Pinillos, M. T. *J. Chem. Soc., Chem. Commun.* **1984**, 936.

(19) Sanger, A. R. *Inorg. Chim. Acta* **1985**, *99*, 95.

(20) Schoettel, G.; Vittal, J. J.; Puddephatt, R. J. *J. Am. Chem. Soc.* **1990**, *112*, 6400.

(21) (a) Usón, R.; Forniés, J.; Tomás, M.; Casas, J. M.; Cotton, F. A.; Falvello, L. R. *Inorg. Chem.* **1986**, *25*, 4519. (b) Cotton, F. A.; Falvello, L. R.; Usón, R.; Forniés, J.; Tomas, M.; Casas, J. M.; Ara, I. *Inorg. Chem.* **1987**, *26*, 1366. (c) Usón, R.; Forniés, J.; Tomás, M.; Usón, I. *Angew. Chem., Int. Ed. Engl.* **1990**, *29*, 1449.

(22) (a) Sokolov, V. I.; Bashilov, V. V.; Anishchenko, L. M.; Reutov, O. A. *J. Organomet. Chem.* **1974**, *71*, C41. (b) Crespo, M.; Rossell, O.; Sales, J.; Seco, M. *J. Organomet. Chem.* **1984**, *273*, 415.

(23) Wojnowski, W.; Wojnowski, M.; von Schnering, H. G.; Noltemeyer, M. *Z. Anorg. Allg. Chem.* **1985**, *531*, 153.

Scheme 1
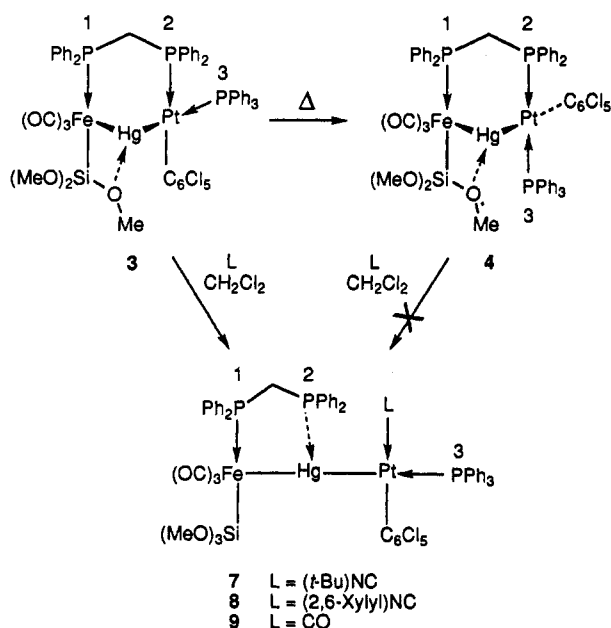
ligands on the Pt—X bonds.[24] Possible phosphine cata-lyzed mechanisms for their *cis/trans* isomerizations have been discussed, involving pentacoordinated intermedi-ates.[25] The very similar spectroscopic properties of **3** and **4** are consistent with the presence of a comparable metal core in these complexes. The $^2J(P^1-P^2)$ and $^4J(P^1-P^3)$ couplings are almost unaffected by this transformation; the $^2J(P^2-P^3)$ coupling however be-comes very large (391 Hz), indicating a mutual *trans* position of P^2 and P^3. Compared to **3** the $J(P-^{199}Hg)$ couplings of P^1 and P^2 of **4** remain comparable; however, the $^2J(P^3-^{199}Hg)$ coupling of only 220 Hz (contrasting with the value of 2867 Hz in **3**) indicates a *cis* position of P^3 with respect to the platinum-bound Hg atom. The $^1J(^{199}Hg-^{195}Pt)$ coupling constant of 6300 Hz is smaller than that in **3**, suggesting a weakening of the Pt—Hg bond. An increase of $^1J(P-^{195}Pt)$ coupling constants of P^2 and P^3 (by 375 and 382 Hz, respectively) is observed in going from **3** to **4**, indicating a strengthening of the P—Pt bonds. These lower $J(Hg-Pt)$ and $J(P-Pt)$ cou-plings in **4** compared to **3** could be the result of a higher *trans* influence of the Pt—Hg bond and of the C_6Cl_5 group compared to that of the phosphine ligands, possibly reflecting the unusual bridging situation of the mercury atom.

The formation of **7—9** from **3** may be explained by a simple displacement of the dppm ligand on platinum by L (L = CO, RNC) leading to the chain structure Fe—Hg—Pt (discussion of the geometry vs spectroscopic data, see below). Interestingly, no reaction was ob-served when L was added to the thermodynamically more stable **4** (Scheme 1). This could be the result of a P—Pt bond strengthening, consistent with the changes in the $^1J(Pt-Hg)$ and $^1J(P-Pt)$ coupling constants of **4** when compared to **3** (see above). Even excess PPh3 did not react with **3** to yield a complex of type **7—9**, which could be due to steric reasons. A possible reversibility of the formation of **9** could be indicated by the fact that,

even after bubbling CO through a solution of **3** for 1 h, a minor quantity of the starting material was still found in the $^{31}P\{^1H\}$ NMR spectrum.

The structural relationship between **3** and *mer*-[(OC)3-{(MeO)3Si}Fe(μ-dppm)PtH(PPh3)] (**5**)[3a] suggested the possibility of replacing the proton on platinum by the isolobal [Hg(C_6Cl_5)]$^+$ cation (eq 7). However, the main product of this reaction was **6** and the formation of some **4** was evidenced by $^{31}P\{^1H\}$ NMR. Addition of **5** to a solution of [Hg(C_6Cl_5)]$^+$ at −30 °C yielded more **4** but complex **6** was still predominant. Interestingly, no formation of **3** was observed in these reactions (it would have been stable under these low temperature condi-tions), indicating a direct pathway to **4**.

Although it is difficult to draw definite conclusions about the exact structure of complexes **3** and **4** without structural data, the proposed geometry with a lightly stabilized Hg atom bridging two different transition metals fits best with their spectroscopic data and observed reactivities. A strictly linear FeHgPt array that would correspond to the usual linear coordination of mercury appears incompatible with the presence of a bridging dppm ligand, since the Fe—Pt separation would have to be superior to 5 Å. It is interesting that linear Os—O—Os (d(Os—Os) = 3.584(2) Å)[26a] and Re—O—Re (d(Re—Re) = 3.820(2) Å)[26b] arrays have been structurally characterized in doubly bridging dppm complexes where no distortion of the dppm backbone was observed owing to the smaller size of the atom in the middle of the chain. Large intramolecular distances in binuclear dmpm- and dppm-bridged complexes were reported in [Me3Pt(μ-I)(μ-dmpm)2PtMe3] (d(Pt—Pt) = 4.707(1) Å)[26c] and in [((C_6H_4Me-o)2Pt(μ-dppm)2PtMe2] (d(Pt—Pt) = 4.91 Å).[26d] An interesting "model" for **3** or **4** could be the structurally characterized complex **10** (see below), as their $^{31}P\{^1H\}$ NMR spectroscopic data show striking similarities. Thus, the small $^3J(P-^{195}Pt)$ con-stant of ca. 10 Hz of the iron-bound phosphorus atom, the small $^{2+4}J(P^1-P^2)$ coupling of 27 Hz between the dppm phosphorus atoms, and all three $^2J(P-^{117,119}Sn)$ coupling constants in **10** corresponding to the $^2J(P-^{199}$-Hg) couplings in **4** are similarities worth mentioning.

Another interesting question concerns the origin of the Fe—Hg—*Pt*—C_6Cl_5 array in **3** obtained according to eq 5. Why did nucleophilic attack of the Pt—Cl bond of *trans*-[ClPt*Hg*(C_6Cl_5)(PPh3)2] (itself formed by an inser-tion reaction of [Pt(C_2H_4)(PPh3)2] into [HgCl(C_6Cl_5)]6) by **1** not lead to a Fe—Pt—*Hg*—C_6Cl_5 array, as previously observed with other carbonyl metalates?[2d] A major rearrangement has occurred, possibly with Hg deinser-tion/reinsertion into the Fe—Pt bond, which resulted in positional isomerism and formation of the Fe—Hg—*Pt*—C_6Cl_5 array. Precedents for demercuriation of com-plexes of type Pt(HgR)R′(PPh3)2 are known, and related organic group transfer reactions between [PtCl2(CO)L] and [HgR2] giving [PtClR(CO)L] have been studied.[22b,27] However, the spectroscopic data available for the start-ing material [ClPt*Hg*(C_6Cl_5)(PPh3)2] and the absence of

(24) (a) Appleton, T. G.; Clark, H. C.; Manzer, L. E. *Coord. Chem. Rev.* **1973**, *10*, 335. (b) Hartley, F. R. *J. Chem. Soc. Rev.* **1973**, *2*, 163.
(25) MacDougall, J. J.; Nelson. J. H.; Mathey, F. *Inorg. Chem.* **1982**, *21*, 2145.

(26) (a) Chakravarty, A. R.; Cotton, F. A.; Schwotzer, W. *Inorg. Chem.* **1984**, *23*, 99. (b) Bartley, S. L.; Dunbar, K. R.; Shih, K.-Y.; Fanwick, P. E.; Walton, R. A. *J. Chem. Soc., Chem. Commun.* **1993**, *98*. (c) Ling, S. S.; M. Jobe, I. R.; Manojlovic-Muir, L.; Muir, K. W.; Puddephatt, R. J. *Organometallics* **1985**, *4*, 1198. (d) Hutton, A. T.; Pringle, P. G.; Shaw, B. L. *J. Chem. Soc., Dalton Trans.* **1985**, 1677.
(27) Cross, R. J.; McLennan, A. J. *J. Organomet. Chem.* **1983**, *255*, 113.

Table 10. $^{31}P\{^1H\}$ and IR Data for Complexes $[(OC)_3\{(MeO)_3Si\}Fe(\mu\text{-dppm})HgX]^{3f}$

	$\delta(^{31}P\{^1H\})$		J/Hz			IR/cm^{-1}
	P^1	P^2	^2J(P^1–P^2)	^2J(P^1–Hg)	^1J(P^2–Hg)	ν(CO)(KBr)
[(OC)$_3${(MeO)$_3$Si}Fe(μ-dppm)HgCl]	55.7	–0.5	136	460	1745	2020 (m), 1980 (sh), 1960 (vs)
[(OC)$_3${(MeO)$_3$Si}Fe(μ-dppm)HgI]	61.1	–4.9	135	418	1595	
2	61.8	–16.1	134	244	600^a	2015 (m), 1944 (vs br)
[(OC)$_3${(MeO)$_3$Si}Fe(μ-dppm)HgC$_6$H$_5$]	56.7	–20.9	115	29	360	2003 (m), 1941 (sh), 1923 (vs)

^{a} Determined by ^{199}Hg$\{^1H\}$ NMR.

a crystal structure do not unambiguously rule out a [ClHg*Pt*(*C₆Cl₅*)(PPh₃)₂] arrangement, which would make the results of eq 5 easier to understand. On the other hand, the spectroscopic data available for the known complexes *cis*-[m–Pt–*Hg(C₆Cl₅)*(PPh₃)₂] (m = metal carbonyl fragment), which were also obtained from *trans*-[ClPt*Hg(C₆Cl₅)*(PPh₃)₂] (eq 3),[2d] do not, a posteriori, unambiguously rule out the presence of a m–Hg–Pt array in these complexes. Furthermore, the spectroscopic data for the (structurally characterized) m–Hg–Pt[2a] and (proposed) m–Pt–Hg arrays[2d] show striking similarities. The X-ray structure determination of the parent complex [ClPt*Hg(C₆Cl₅)*(PPh₃)₂] should therefore help to solve this problem.

Structural vs Spectroscopic Data for 2 and 7–9. From the observed spectroscopic data (Table 6) we propose for **8** and **9** structures analogous to that established for **7** which indicates an uncoordinated P² atom of the dppm ligand. However, couplings of the type ^1J(P²–^{199}Hg), ^2J(P²–^{195}Pt), and ^3J(P²–P³) were unambiguously evidenced in solution (Table 6). All coupling constants were observed at room temperature and no change of the spectrum was found when the temperature was decreased, ruling out a fluxional process being responsible for the observed phenomenon. We have observed a similar effect in *mer*-[(OC)₃Fe(μ-dppm)(SnClPh₂)₂] which contains a semibridging dppm ligand.[28]
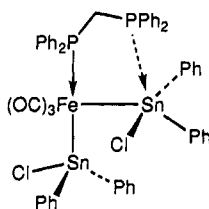
As for **7** the structural data suggested no bonding interaction between P and Sn (d(P–Sn) = 3.140(2) Å); however a significant ^1J(P–^{117,119}Sn) coupling of 85 Hz was found in the $^{31}P\{^1H\}$ NMR spectrum. To the best of our knowledge there have been no reported examples of such discrepancies between solid-state structures and solution spectroscopic data in heterometallic dppm-bridged complexes. The pendant nature of a monohapto dppm could mimic weak interactions with monodentate ligands that could not be characterized otherwise. In the recently reported dimer [(R₂P)Hg(μ-PR₂)₂Hg(PR₂)] (R = SiMe₃) a P–Hg distance of 3.246(1) Å was found (sum of the van der Waals radii: 3.35 Å).[29] This interaction did not influence the linearity of the P–Hg–P array, and the long P→Hg bridge was attributed to a weak dative interaction. In contrast to our case, NMR

spectroscopy did not suggest a P–Hg interaction and this was explained by dissociation in solution.

Further comparisons are provided in Table 10 where the $^{31}P\{^1H\}$ NMR and IR spectroscopic data in the ν-(CO) region of several dppm-bridged FeHgX (X = Cl, I, C₆Cl₅ (**2**), C₆H₅) complexes are collected. Obviously, the electronegativity of X strongly influences the chemical shift values δ and the ^1J(P–^{199}Hg) coupling constant. We found that on going from X = Cl to X = C₆H₅ the chemical shift value of the Hg-bound phosphorus atom varies from δ –0.5 to –20.9 and therefore approaches the value of the uncoordinated situation of a dppm-*P* ligand (the uncoordinated phosphorus atom of a pendant dppm ligand is observed at δ –23). Simultaneously, the ^1J(P–^{199}Hg) coupling constant decreases considerably from 1745 to 360 Hz.

The ^1J(P–^{199}Hg) coupling constant of 600 Hz observed in the $^{31}P\{^1H\}$ NMR of **2** is comparable to the observed values in **7–9**. There should be a direct correlation of δ and J(P–Hg) values with the P–Hg distances observed in the solid state. Indeed, the P–Hg distance of 3.17 Å found in **2** is very long for a bonding interaction, although shorter than in **7**, which is in accordance with spectroscopic data.

Complexes Containing Platinum and Tin. Metal–metal bonded complexes associating platinum and tin have been of considerable interest since the discovery of highly active hydrogenation and hydroformylation catalysts based on the PtCl₂(PR₃)₂/SnCl₂ system.[30] The isolation and study of new heterometallic complexes containing tin chloride and platinum could therefore help to improve our understanding of such systems.

Platinum–tin complexes often display, when isolated, very complicated rearrangement reactions.[31] SnCl₂ can act as a Lewis acid,[32] or insert into a M–Cl bond to form SnCl₃⁻ as a ligand or as a counterion. The ligand SnCl₃ is known to exhibit a *trans* influence similar to the one of Cl but has a strong *trans* effect due to its high π-back-bonding capacity. Recently, the dissociation–association mechanism of SnCl₂ has been studied in detail for complexes of the type (R₃P)₂PtCl(SnCl₃) (R = tolyl).[31a] In the latter complex the SnCl₂ group was suspected to move in and out of a Pt–Cl bond, accounting for a *cis/trans* isomerization of the complex. By comparison, two different initial steps could be envisaged for the formation of **10** (Scheme 2): (i) a Fe–Sn bond is initially formed upon the nucleophilic attack of **1** at the –SnCl₃ group; (ii) first a nucleophilic attack of **1** at the Pt–Cl unit occurs, and subsequently, the SnCl₂ fragment moves out of the Pt–Cl bond to insert into the newly formed Fe–Pt bond.

(28) Braunstein, P.; Knorr, M.; Strampfer, M.; DeCian, A.; Fischer, J. *J. Chem. Soc., Dalton Trans.* **1994**, 117.

(29) Goel, S. C.; Chiang, M. Y.; Rauscher, D. J.; Buhro, W. E. *J. Am. Chem. Soc.* **1993**, *115*, 160.
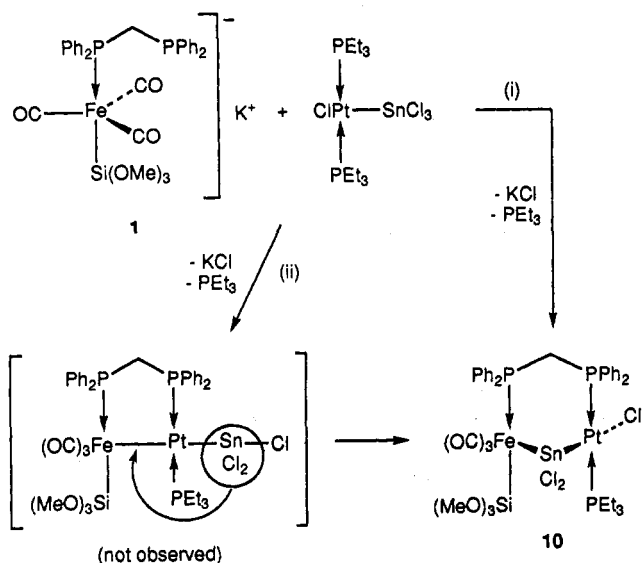
(30) (a) Hsu, C. Y.; Orchin, M. *J. Am. Chem. Soc.* **1975**, *97*, 3553. (b) Gómez, M.; Muller, G.; Sainz, D.; Sales, J. *Organometallics* **1991**, *10*, 4036 and references cited therein.

(31) (a) Rüegger, H.; Pregosin, P. S. *Inorg. Chem.* **1987**, *26*, 2912. (b) Holt, M. S.; Wilson, W. L.; Nelson, J. H. *Chem. Rev.* **1989**, *89*, 11.

(32) Chann, D. M.; Marder, T. B. *Angew. Chem., Int. Ed. Engl.* **1988**, *27*, 442.

Scheme 2

(not observed)   **10**

It is well-known that $SnCl_2$ inserts into the metal–metal bond of organometallic complexes and a variety of complexes with m–$(SnCl_2)$–m[33a] and m–$(SnCl_2)$–m'[33b] (m, m' = transition metal carbonyl fragments) arrays have been described. Although only few such complexes have been structurally characterized, like $[Ir_2(\mu\text{-}SnCl_2)\{\mu\text{-}Ph_2P(CH_2)_4PPh_2\}_2(CO)_2Cl_2]$[34b] or $[Mn_2(\mu\text{-}SnPh_2)_2(CO)_6\{\mu\text{-}(EtO)_2POP(OEt)_2\}]$,[34c] not many com-

plexes containing dppm and a bridging Sn(II) group between two metal centers have been reported[33c,d] and the crystal structure of complex **10** is a rare example for a stannylene group bridging two different metals.[35]

Supplementary Material Available: Tables of atomic coordinates including H-atom coordinates, thermal parameters and complete listings of bond distances and angles for the structures of **2**, **7**·CH_2Cl_2 and **10**·CH_2Cl_2 (27 pages). Ordering information is given on any current masthead page.

OM9308708

(33) (a) Mackay, M. M.; Nicholson, B. K. In *Comprehensive Organometallic Chemistry* Wilkinson, G., Stone, F. G. A., Abel, E. W., Eds.; Oxford: England 1982; Chapter 43. (b) Behrens, H.; Görting, K.; Merbach, P.; Moll, M. *Z. Anorg. Allg. Chem.* **1979**, *454*, 67. (c) Faraone, F.; Bruno, G.; Lo Schiavo, S.; Bombieri, G. *J. Chem. Soc., Dalton Trans.* **1984**, 533. (d) Sanger, A. R. *Inorg. Chim. Acta* **1992**, *191*, 81.

(34) (a) Balch, A. L.; Olmstead, M. M.; Oram, D. E.; Reedy, P. E., Jr.; Reimer, S. H. *J. Am. Chem. Soc.* **1989**, *111*, 4021. (b) Balch, A. L.; Davis, B. J.; Olmstead, M. M. *Inorg. Chem.* **1990**, *29*, 3066. (c) Carreño, R.; Riera, V.; Ruiz, M. A.; Jeannin, Y.; Philoche-Levisalles, M. *J. Chem. Soc., Chem. Commun.* **1990**, 15.

(35) See for example: (a) Nesmeyanov, A. N.; Anisimov, K. N.; Kolobova, N. E.; Zakharova, M. Ya. *Izv. Akad. Nauk SSSR, Ser. Khim.* **1965**, 1122. (b)Thomson, L. K.; Eisner, E.; Newlands, M. J. *J. Organomet. Chem.* **1973**, *56*, 327.